

Visaveliya, Nikunj Kumar R.; Köhler, Michael

Softness meets with brightness: dye-doped multifunctional fluorescent polymer particles via microfluidics for labeling

Original published in: Advanced optical materials. - Weinheim : Wiley-VCH. - 9 (2021), 13, art. 2002219, 22 pp.
Original published: 2021-05-04
ISSN: 2195-1071
DOI: [10.1002/adom.202002219](https://doi.org/10.1002/adom.202002219)
[Visited: 2022-02-25]



This work is licensed under a [Creative Commons Attribution 4.0 International license](https://creativecommons.org/licenses/by/4.0/). To view a copy of this license, visit <https://creativecommons.org/licenses/by/4.0/>

Softness Meets with Brightness: Dye-Doped Multifunctional Fluorescent Polymer Particles via Microfluidics for Labeling

Nikunj Kumar R. Visaveliya* and Johann Michael Köhler*


Fluorogenic labeling strategies have emerged as powerful tools for *in vivo* and *in vitro* imaging applications for diagnostic and theranostic purposes. Free organic chromophores (fluorescent dyes) are bright but rapidly degrade. Inorganic nanoparticles (e.g., quantum dots) are photostable but toxic to biological systems. Alternatively, dye-doped polymer particles are promising for labeling and imaging due to their properties that overcome limitations of photodegradation and toxicity. This progress report, therefore, presents various synthesis techniques for the generation of dye-doped fluorescent polymer particles. Polymer particles are relatively soft compared to inorganic nanoparticles and can be synthesized with characteristics like biocompatibility and stimuli responsiveness. Also, their ability of loading fluorophores through various interactions reveals brightness. Here, a multiscale-multicolor library of bright and soft fluorescent polymer particles is generated hierarchically. Various microfluidic supported strategies have been applied where fluorophores can be linked to polymeric networks noncovalently and covalently in the interior, and at the surface of nanoparticles (60–550 nm). Besides, microfluidic strategies for hydrophilic and hydrophobic fluorescent polymer microparticles (20–800 μm) have been performed for systematic tuning in size and color combination. Furthermore, soft and bright particulate assemblies are enabled through interfacial interactions at the intermediate scale (600 nm–3 μm) between the nanometer and micrometer lengthscale.

1. Introduction

The advancement in the field of biophotonics and chemical biology has allowed significant progress in the understanding

Dr. N. R. Visaveliya, Prof. J. M. Köhler
Department of Physical Chemistry and Microreaction Technology
Institute for Chemistry and Biotechnology
Technical University of Ilmenau
98693 Ilmenau, Germany
E-mail: michael.koehler@tu-ilmenau.de

Dr. N. R. Visaveliya
Department of Chemistry and Biochemistry
The City College of The City University of New York
New York, NY 10031, USA
E-mail: nvisaveliya@ccny.cuny.edu

 The ORCID identification number(s) for the author(s) of this article can be found under <https://doi.org/10.1002/adom.202002219>.

© 2021 The Authors. Advanced Optical Materials published by Wiley-VCH GmbH. This is an open access article under the terms of the Creative Commons Attribution License, which permits use, distribution and reproduction in any medium, provided the original work is properly cited.

DOI: 10.1002/adom.202002219

of cellular activities and functions together with disease diagnosis and their origin at the sub-cellular level.^[1–4] Suitable detection techniques and efficient materials are demanded that can convert chemical and biochemical signals into optical readouts.^[5–9] In this regard, fluorogenic labeling strategies by using fluorescent materials (optical agents) are very promising.^[10–13] Fluorescent materials can spontaneously re-emit light after excitation by absorption of energy from the source of an external electromagnetic field.^[12] The emission range of fluorescent materials in a broad spectrum of fluorescent colors makes them stronger candidates for detailed and progressive analysis during their applications as labels.^[14–16] In general, fluorescence-based labeling techniques, owing to their high sensitivity, speed, resolution, and specificity, are powerful tools for the detection and analysis of complex biological and materials systems based on light-matter interactions.^[7,10–11,17]

For efficient outcomes in the form of fluorescence yield, labeling materials are required to be bright and photostable. Fur-

thermore, their properties such as superior chemical inertness, biocompatibility, nonblinking, low photobleaching, and lower cytotoxicity make them suitable for biophotonics applications.^[18] Usually, the application of fluorescent dyes is mainly the focus of interest for molecular labeling in chemical and biomedical diagnostics, histology, and cell technology.^[15,19–21] Fluorescent dyes are advantageous because of their lower cost, ease of clearance, high sensitivity, brightness, and feasibility of multicolor labeling.^[15,22] Improvements of well-known fluorescent dyes (fluorophores) and further progress in new ones with a broader range of colors can provide extensive diversity in detection systems with enhanced sensitivity.^[23–26] However, many of the applied methods suffer from incompatibilities of chemical and biological systems with the dyes.^[27] Also, the quick degradation of dyes by interaction with the chemical environment is a major concern.^[28] Besides, inorganic nanoparticles (for instance, quantum dots) are equally powerful optical agents because of their superior brightness, photostability, chemical stability, and robustness.^[29–32] However, the class of inorganic nanoparticles is also relatively less effective in biophotonics because of their disadvantages including toxicity issues of quantum dots and

upconversion nanoparticles and short excitation and emission wavelengths of silica nanoparticles and carbon dots.^[33–34] Alternatively, dye-doped fluorescent polymer particles are very promising because they can overcome the issues of photochemical degradation (e.g., of dyes) and cytotoxicity (e.g., of quantum dots).^[18,35–42] Furthermore, fluorescent polymer particles can be tailored with additional advantages such as biocompatibility, longer fluorescence lifetime, large absorption coefficients, and multicolor labeling ability that make them suitable optical agents for labeling of biological as well as materials systems.^[36]

Most of the types of polymers can be classified as amorphous (as well as semi-crystalline) and insulating materials.^[43] They are usually not conducting the electricity, not interacting with light, and hence do not appear to absorb and reemit the light (fluorescence). However, specific types of polymer particles are highly suitable and nontoxic for biological systems because of their excellent biocompatibility, stimuli responsiveness, cross-linking variability, and cargo-carrying ability.^[44–48] Furthermore, the merging of bright fluorophores with polymer particles allows them to use as potential optical agents.^[36] In this way, the combination of the fluorescent property of fluorophores and biocompatibility of polymer particles can create powerful fluorescent labels that are prerequisites for fluorescence-based biological and biomedical applications. Since fluorescent polymer particles are promising candidates for labeling, the key challenges during their formation need to be addressed. Some of those challenges are obtaining their size homogeneity, efficient linking of fluorophores to prevent leaking, prevention of aggregation caused quenching of fluorophores in the polymer matrix, and desired surface properties of particles for interfacial interactions with targeted sites.^[36,41,49–52] For obtaining the homogeneous polymer particles together with their size hierarchy and tunability, microfluidic-mediated reaction techniques are advantageous.^[53–56] Microfluidics can provide a platform for efficient reactant mixing, variability in reactants composition in a continuous flow, and high surface area.^[57–64] Overall, with all of these advantages, the uniform product outcome can be realized. The fluorophore leaking concern can be solved by covalent linking of fluorophores in the interior, and at the surface of nanoscale polymer particles through bioconjugations.^[35] Likewise, systematic size-tunable microscale polymer particles with their hydrophilic and hydrophobic characteristics can also be produced by droplet microfluidics.^[42,65–66] Also, a wide variety of color combinations can be introduced in microparticles continuously on a single platform by arranging an integrated microfluidic setup.^[42] Not only single types of nanoscale and microscale polymer particles but structurally hierarchical particulate assemblies of various types of tunable fluorescent polymer particles can be produced through interfacial interactions.^[67] Furthermore, additional particulate properties such as particle shapes, porosity, and surface wrinkling can also be fabricated upon requirements for optimized optical signals due to efficient interactions with the targeted site.^[66]

Overall, fluorescent polymer particles are promising for labeling biological and materials systems. The scope of this progress report is to summarize and review the research from the authors' laboratory regarding the microfluidic supported engineering of multiscale and multicolored dye-doped fluorescent polymer particles of high quality by addressing critical

challenges during their syntheses. Initially, a particle-based labeling concept and advantages of fluorescent polymer particles for labeling are explained. Subsequently, microfluidic synthesis techniques for nano- and microparticles are explained. In the nanoscale regime, various strategies for linking fluorophores with polymer particles are described by controlling various properties such as low polydisperse size, stability, and surface functionality. For the microscale particles, a functionalized microreactor supported microfluidic arrangement has been used to produce hydrophilic and hydrophobic fluorescent polymer microparticles with a wide range of various color combinations. Furthermore, in situ assemblies of the fluorescent polymer particles at the intermediate length scale between higher nanometer and lower micrometer were presented in the hierarchical order. In the last, the size and color-based concept of an extensive hierarchical approach for labeling various materials systems has been proposed. The main focus here is to review the research of the authors' laboratory about synthesis strategies of fluorescent polymer particles only.

2. Labeling Strategy Based on Fluorescent Polymer Particles

2.1. A General Labeling Concept

Intracellular tracking of biomolecules (amino acids, peptides, proteins, and antibodies) in the biological systems often requires labeling with a reporter or sensor.^[11,68] For instance, fluorescent amino acid and fluorescent nucleobase are versatile building blocks that can be applied to the targeted site for fluorescence imaging.^[69–70] Similarly, green fluorescent proteins can be applied to a region of the targeted protein environment, and hence their activities can be analyzed by fluorescence imaging.^[71] Usually, a wide range of various fluorescent dyes is utilizing as fluorescent markers owing to their brightness and full color/emission range.^[15,22] While molecular labeling is highly useful for diagnosing and tracking the activities of organelles and biomolecules at a much smaller length scale,^[72] the labeling with particulate fluorophores allows the imaging of cells, tissues, and extracellular matrix within biological systems through the interfacial interaction-based approach.^[73–74] In this regard, particulate fluorophores such as quantum dots, lanthanide-doped nanoparticles, conjugated polymer nanoparticles, fluorescent silica nanoparticles, etc. are promising components.^[75–78] Though they are efficient and prominent candidates for labeling purposes, some of the key demerits and limitations such as cytotoxicity, low photostability, and quenching can hinder them from safe and sustained uses for biological systems. Alternatively, surface-functionalized dye-doped fluorescent polymer particles^[36,79–81] are highly promising for safe use for biological labeling because of their biocompatibility, nontoxicity, and longer fluorescence lifetime (**Figure 1A**).

2.2. Advantage of Polymers

Polymers are soft and relatively flexible compared to hard metal nanoparticles, for instance. Supramolecular polymers

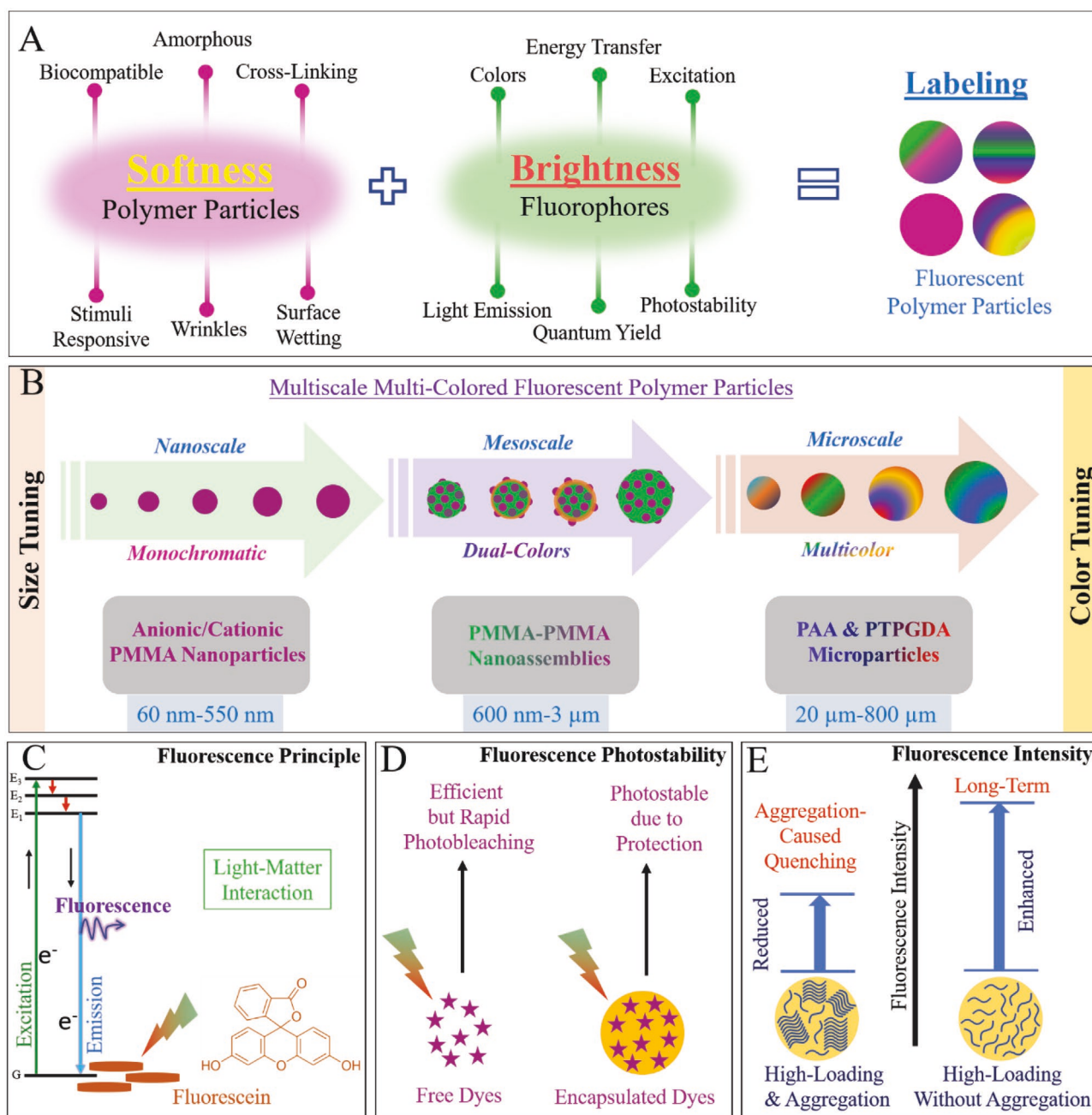


Figure 1. Schematic overview of the multiscale multicolored fluorescent polymer particles. A) Synergistic properties of soft polymer particles and bright fluorophores make fluorescent polymer particles suitable for labeling applications. B) Multiscale multicolored synthesis of fluorescent polymer particles: nanoscale polymethylmethacrylate (PMMA) particles of size range 60–550 nm through emulsion polymerization, mesoscale PMMA-PMMA nanoassemblies of size range 600 nm–3 μm through electrostatic interactions during emulsion polymerization, and microscale polyacrylamide and poly(tripropylene glycol diacrylate) (PTPGDA) particles of size range 20–800 μm through photopolymerization. C) A general principle of fluorescence in which excited electrons emit the fluorescence light upon returning to the ground state. D) Photostability comparison of fluorophores outside and inside of the particles. E) A basic concept for comparison of fluorescence intensity and quenching of the fluorophores dispersed inside the polymer particle.

reveal fascinating properties such as exogenous and endogenous stimuli responsiveness and reversibility that is regulated by the assembly-disassembly process through their noncovalent connections, on the one side.^[8,44,46,82] Cross-linked covalent polymers, on the other side, are very useful because they allow introducing molecular functionalities in their covalent network.^[43,83–84] Most polymers are composed of carbon,

hydrogen, oxygen, and nitrogen in their macromolecular backbone and network. Moreover, side chains of the backbone may contain several functional groups such as hydroxyl, carboxylic acid, ester, amine, and amide.^[43] Most of these elements and functional groups are compatible with biological systems that are prerequisites for using them in biomedical applications, and hence selective types of polymeric networks can also be

called synthetic bio-analogous materials.^[85–86] The particulate polymers are particularly interesting because of their interior structure and surface functionality.^[87] The key physicochemical and interfacial characteristics of polymer particles such as swellability, soft interior and interface, size and shape tunability, porosity, and biodegradability make them powerful and promising components as carriers for drug delivery and scaffolds for tissue engineering.^[46,82] Also, the merging of suitable fluorophores in the interior or at the surface of polymer particles by various chemical interactions allow them to potentially and safely use as fluorescent labels for imaging and theranostics applications.^[35–36,42,88]

2.3. Fluorescent Polymer Particle-Based Labeling: Softness of Polymer Particles and Brightness of Dyes

The difficulties of chemical degradation of free dyes and toxicity of quantum dots as labels for biological systems can be overcome by the application of combinatorial constructed dye-doped polymer particles.^[89–92] Following this concept, only a very low amount of dyes is required inside the polymer particles because they can be applied universally and independently from the specific properties of the surrounding medium. When only free dyes (without doping in polymer particles) are utilized for labeling purposes, their molecular structure, solubility, adhesion or repelling properties, specific interaction with targeted sites, and chemical resistivity for acids, bases, enzymes, and other aggressive factors are required to be controlled. But, when dyes are embedded inside the polymer particles, all of these features can be controlled by the polymer matrix (interior) and the surface of the polymer particles. Embedding the dyes inside the particles means that they are safely encapsulated and suitable for biological applications as far as biocompatible properties can be controlled by the polymer matrix.^[36] The performed trick is the de-coupling of chemical challenges in the application of labels from their optical function. As a result, both properties can be optimized independently from each other (Figure 1A).

The application of polymer particles for labeling is mainly determined by two factors: i) size-compatibility with the labeled object and ii) detectability by a suited optical readout system. The size spectrum of dye-doped polymer particles can cover, principally, the whole range from nanometer up to micrometer and millimeter length scale. A brief classification of the size hierarchy of polymer particles based on the scope of this review article is illustrated in Figure 1B. Nanoscale polymer particles can be formed via various polymerization techniques such as emulsion polymerization, suspension polymerization, and miniemulsion polymerization.^[93–94] Besides, polymer micro-particles of tunable size can be produced via photopolymerization techniques.^[42,65] The size of polymer particles, for example, about 30 nm is large in comparison with single molecules, but small in comparison with cells. Small cells as *Escherichia coli* (*E. coli*), for example, have a cell volume of about three femtoliters (10^{-15} L).^[95] The volume of small polymer particles can be considered in the range of some tens of zeptoliters (10^{-21} L), which means less than 0.01% of the mentioned bacteria cell. From this point of view of size relation, it can be imagined that dye-doped particles are not the perfect choice for undisturbed

labeling of single molecules or molecular structures. But, besides this special case, they can be applied for all labeling purposes on objects starting with sizes of small bacterial cells, cell organelles, or even supermolecular intracellular structures. The size of particles can be an important parameter for optical recognition and measurements, too.^[96–97]

For pigment dyes, the optical determination of absorbance and, therefore, the identification of color is dependent on the substance-specific extinction coefficient, dye concentration, and the optical path length of the particle-crossing beam.^[98–100] The maximum concentration of dyes can be in the order of magnitude of about 0.1 M in dye-doped fluorescent polymer particles. For this concentration, a minimal particle diameter can be estimated for a required minimum absorbance. For small objects, it is desirable to realize an absorbance (extinction) no less than about 0.1 in order to get acceptable signal-to-noise ratios. For a dye with a molar extinction coefficient of 10^4 L mol⁻¹·cm⁻¹, a particle diameter minimum of 1 μm would be sufficient. For lower molar extinction coefficients and lower dye concentration, the particle diameter needs to be enlarged accordingly. Thus, particles of about 100 μm diameter are required if the concentration can only be 10×10^{-3} M and the molar extinction coefficient is about 10^3 L mol⁻¹·cm⁻¹. The brightness of fluorescent particles depends on the number of dye molecules per polymer particle. In general, size is an important aspect that regulates the stability of the particles as well as their surface interactions with targeted objects (e.g., biological systems or materials systems) during their use as labels.^[101] The size of polymer particles can be controlled by utilizing diverse types of interfacial agents ranging from molecular surfactants to ionic as well as nonionic polyelectrolytes and polymers during the polymerization reaction.^[35,102–103] Also, microfluidic techniques are promising for the synthesis of size-tunable polymer particles.^[104] When polymer particles are doped with fluorophores, the effect of particle size on the absorbance can be determined by size characterization techniques.^[101] Dynamic light scattering (DLS) is a commonly used technique for particle size determination.^[105] Dye-doped polymer particles absorb and emit light, hence the scattering of light through DLS measurement can be influenced depending on the optical characteristics of fluorescent particles. Utilization of selective types and appropriate concentration of dyes can avoid the concern of change in size measurement through the DLS method.^[101]

Recent powerful optical systems can detect single fluorescent molecules.^[106–107] Based on the general fluorescence principle, excited electrons of the fluorescent molecules by irradiation of external light emit the fluorescence light upon their return to the ground state (Figure 1C). The embedding of fluorescent dyes inside the polymer matrix can ensure that the quantum yield of dyes is not lowered by chemical degradation due to the interaction with the surrounding medium. Moreover, the effect of photobleaching during the measurement could be reduced by the stabilization of dye inside the polymer matrix (Figure 1D). At this point, it is important to remark that the accuracy and reproducibility of detection of a certain absorbance are strongly dependent on the particle size, too. The precision in the synthesis of particles of a certain size as well as the determination of a certain color is easier in the case of larger particles than in the case of smaller particles. Consequently, the labeling strategy

should not be based on a maximum of intensity levels or a maximum number of extinction steps but should be operated with a well-distinguishable number of levels in the dye concentration inside the particles. However, the covalent binding of dye molecules inside the polymer matrix can ensure the avoidance of aggregation of dye molecules that directly impact the fluorescent intensity during measurements (Figure 1E). Polymer particles are soft and relatively transparent, and they also allow the loading of the tunable concentration of dyes which can able to control the brightness of fluorescent polymer particles. The number of dye molecules per particle usually determines the brightness of the particles that can be calculated by dynamic fluorescence methods.^[51,108–109] While chemical degradation of free dyes can limit their extensive uses for biological systems, their encapsulation in the polymer matrix is advantageous because specific surface chemistries can be tailored at particle surfaces for efficient interaction with cells or tissues. Overall, dye-doped soft and bright fluorescent polymers are potential candidates for labeling applications.

3. Microfluidic-Supported Synthesis Techniques for Fluorescent Polymer Particles

Quality and controlled properties of the fluorescent polymer particles including uniform size, surface functionality, efficient binding of dyes, and color tunability is key for using them as efficient labels.^[36] Overall, the general concept of fluorescent particle-based labeling demands a practicable strategy for the synthesis of particles. Largescale conventional batch polymerization processes may suffer from a concern of inhomogeneity of particles and nonsystematic distribution of fluorophores inside the polymer matrix. Optimistically, the microfluidic concept of particle generation offers a very convenient solution.^[53,55–56,110–113] In microfluidics, small amounts of reactant-carried fluids are flowing in the microscale channel with high accuracy and initiate the chemical reaction.^[114] One of the key advantages of microfluidics is that they provide an excellent platform for efficient reactants mixing in a highly uniform manner.^[115–116] Fast reactant-mixing at an early stage also proceeds with homogeneous chemical reaction throughout and, as a result, the product is obtained homogeneous.^[57] The polymerization process deals with the interaction of immiscible liquids; for instance, the monomer phase (organic) and surfactant contained carrier phase (aqueous). In this regard, microfluidics plays a crucial role in the manipulation of various immiscible liquids largely based on the control of interface processes and with respect to the wetting behavior of the wall materials of microreactors and microchannels.^[115,117–119] Moreover, it is also possible to operate the reaction with narrow residence time distribution in a microfluidics platform that is highly useful for time-sensitive reactions.^[64,117,120] A cross-flow type microreactor setup has been used here for the syntheses of fluorescent polymer particles of nanoscale and microscale together with their assemblies.

Various types of nanoscale fluorescent polymer particles were prepared via emulsion polymerization.^[35] The emulsification has been initiated in the silicon-chip embedded microreactor chamber and further polymerization proceeds externally at the heating block which is pre-setted with polymeri-

zation temperature as shown in **Figure 2A**.^[121] The flow setup is useful for varying the reaction parameters for tuning the nanoparticle's properties such as particle size, surface charge, and shapes.^[64,102] Flow rate, flow rate ratios, surfactant concentration, and tunable composition of various reactants have been operated through the microfluidic setup. Fluorescent dyes were either incorporated inside the interior or anchored at the surface of nanoparticles.^[35] Embedding the dyes inside the interior has been performed during the synthesis in a single-pot. Besides, attaching the dye through covalent-linking at the extended surface of nanoparticles by bioconjugation is conducted postsynthetically. Overall, it can be better suited to say that the nanoparticle syntheses presented in this progress report are semi-microfluidics because emulsification of immiscible liquids is realized in the microreactor, and further polymerization proceeds externally.^[35]

While nanoparticles syntheses are semi-microfluidics, microscale polymer particles of systematic size and color tunability can be obtained via droplet-microfluidics.^[55,122–123] Various types of fluorescent polymer microparticles were prepared via photopolymerization.^[42,65,124] The immiscible carrier phases were applied for the synthesis of hydrophilic and hydrophobic microparticles. Generated droplets of various sizes are polymerized by ultraviolet light, and hence fluorinated ethylene-propylene (FEP) tubing has been used because of its optical clarity and transparency to pass the light.^[65] Droplet sizes and therefore particle sizes can be controlled precisely by flow rates, flow rate ratios, tubing diameter, and surfactant concentration.^[42] Overall, a large range of colored microparticles with various combinations of dyes with their tunable concentrations is possible to produce by droplet microfluidics. General microfluidic setups for the synthesis of hydrophobic and hydrophilic fluorescent microparticles are shown in **Figure 2B,C**, respectively.

Microfluidic supported strategies of the fluorescent polymer particles at the multiscale level are presented here (scope of this review). Besides, various types of fluorescent polymer particles can be synthesized via various preparation methods that have been largely appeared in the literature.^[36,41,125] For instance, nanoprecipitation techniques are useful for encapsulating various active molecular components such as therapeutic drugs and fluorescent dyes inside the polymer matrix.^[126] In particular, nanoprecipitation is promising for laboratory experiments as well as industrial-scale production of nanoparticles that allow the encapsulation of natural and synthetic molecules and hydrophobic, hydrophilic, and amphiphilic compounds in the polymer particles, and also allow controlling the size of nanoscale polymer particles.^[127–130] Charged-controlled nanoprecipitation allows the formation of ultrasmall nanoparticles of sub-20 nm size.^[131–132] Also, various types of biocompatible polymer nanoparticles such as poly (lactic acid), poly(lactic-co-glycolic acid), and other types can be of particular interest for biological applications that can be developed by nanoprecipitation methods.^[133–134]

4. Fluorescent Polymer Nanoparticles

Nanoscale particles possess a high surface-to-volume ratio that is advantageous for efficient interfacial interactions with various

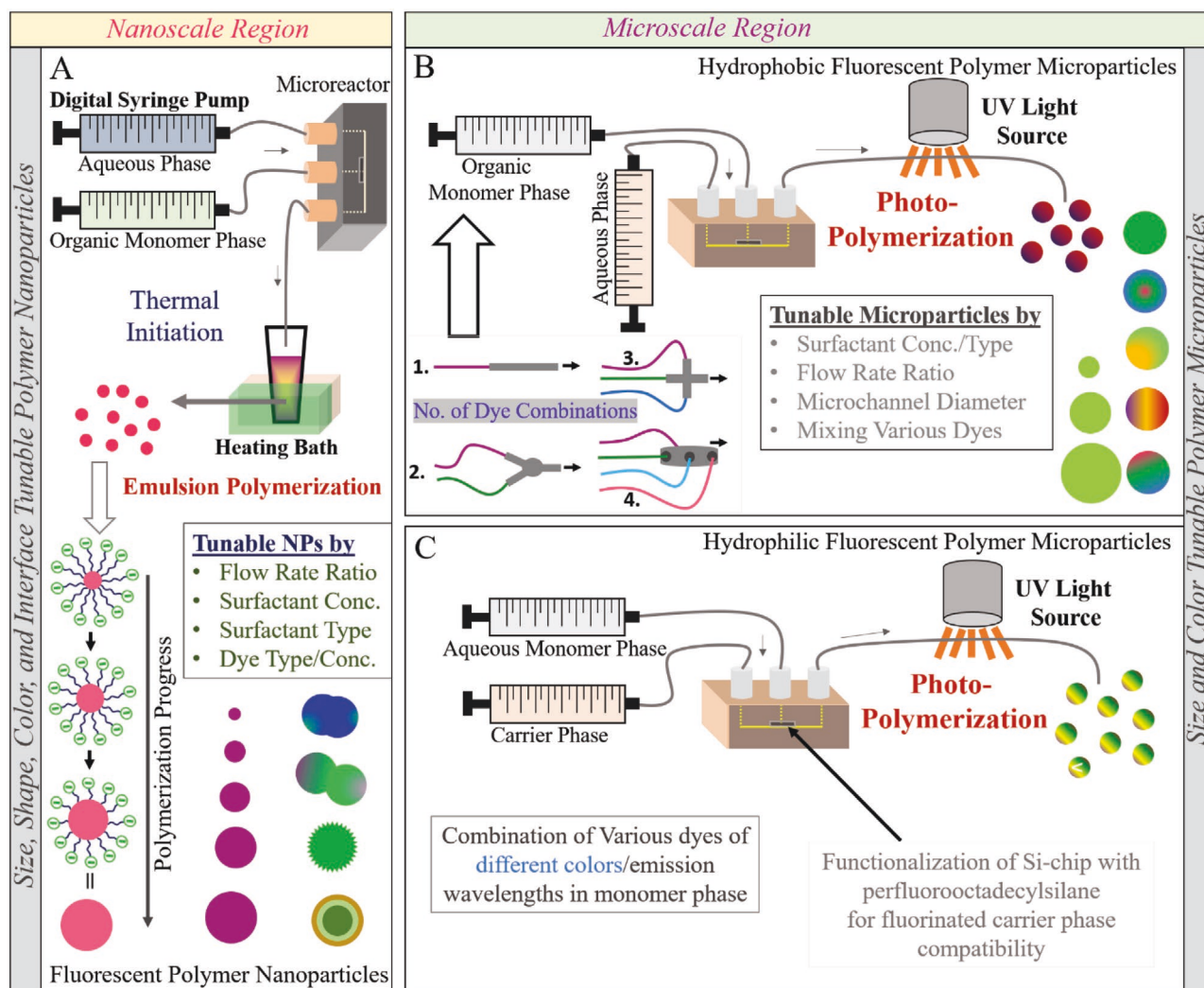


Figure 2. Concepts of microfluidic reaction setups utilized for the synthesis of polymer nanoparticles and microparticles of size and color tunability. A) Setup for size-tunable nanoscale polymer particles via emulsion polymerization in which formation of emulsion takes place in the microreactor and further polymerization proceeds externally at the heating block. B) A general microfluidic setup for hydrophobic microparticles via photopolymerization. C) A microfluidic setup to produce size and color-tuned hydrophilic polymer microparticles via photopolymerization. A) Reproduced with permission.^[35] Copyright 2016, De Gruyter. B) Reproduced with permission.^[42] Copyright 2015, Royal Society of Chemistry. C) Reproduced with permission.^[65] Copyright 2015, American Chemical Society.

active objects.^[135] The flexibility of the covalent cross-linked polymeric network of polymer nanoparticles can accommodate small fluorophores (dye molecules) in the interior.^[131] Also, various hydrophilic dyes can be linked at the surface through chemical reactions. The merging of fluorescent dyes of various emission wavelengths with a polymer network (interior or at the surface) of nanoparticles makes them fluorescence active.^[51] Here, four various synthesis strategies are described with polymethylmethacrylate (PMMA) nanoparticles as a model system.

4.1. Randomly Dispersed Dye-Doped Fluorescent Polymer Nanoparticles

Emulsion polymerization has been performed where two immiscible liquid phases can intermix with the support of an

interfacial agent (surfactant) and subsequently be polymerized to form the polymer nanoparticles.^[136–137] The aqueous carrier phase contains cationic surfactant cetyltrimethylammonium bromide (CTAB) whereas organic dye was dissolved in the monomer dispersed phase. The emulsification of both immiscible phases has been carried out in the microreactor as shown in Figure 2A. Nile red dye^[138] is very bright and here it is chosen as a model fluorescent dye to be incorporated in the polymer matrix. The monomer phase is composed of methylmethacrylate (MMA) monomer, ethylene glycol dimethacrylate (EGDMA) cross-linker, azobisisobutyronitrile (AIBN) thermal initiator, and Nile red fluorescent dye (Figure 3A). When the monomer phase meets with the aqueous solution, the high surface tension can be reduced down by the use of a surfactant.^[139] It can be imagined that the cross-linking network can begin to form upon the initiation of the polymerization process at

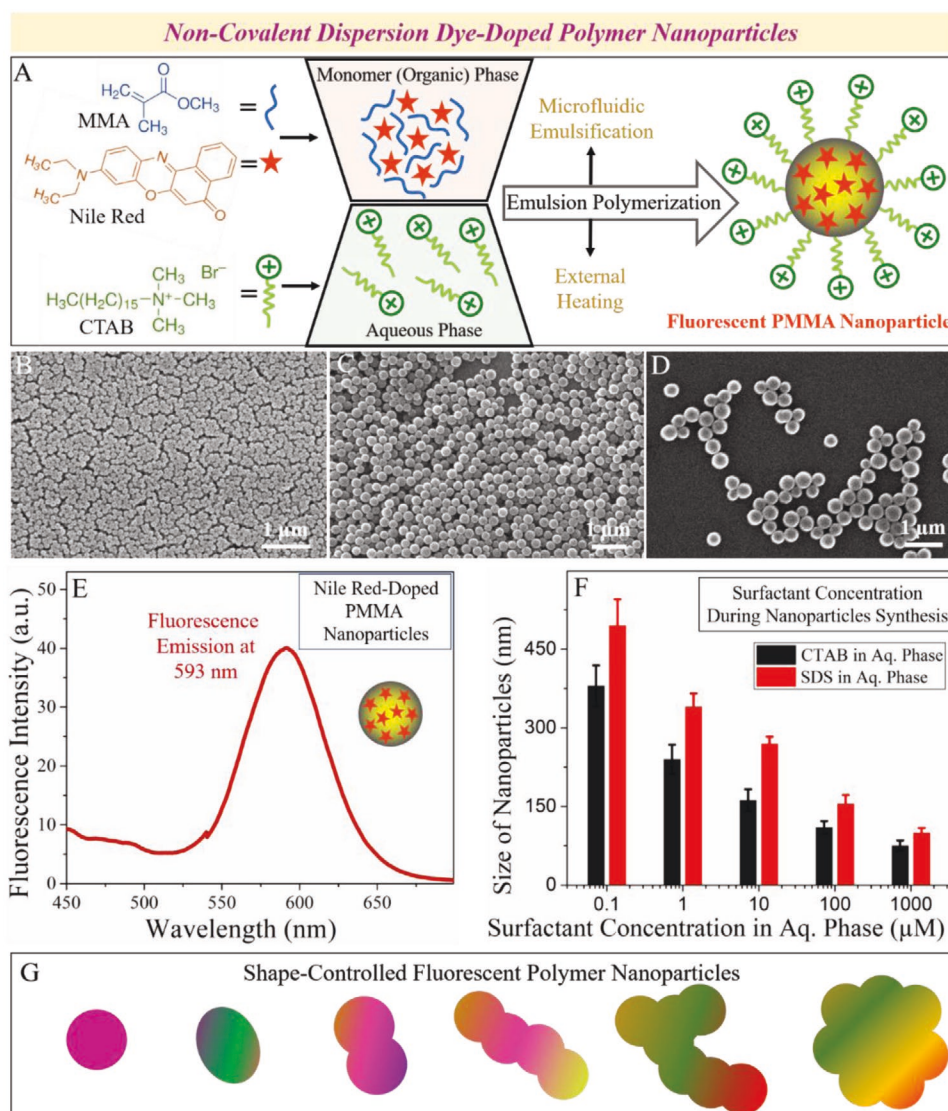


Figure 3. Freely dispersed (noncovalent bonding) dye-doped polymer nanoparticles. A) Synthesis ingredients of the Nile red-embedded cetyltrimethylammonium bromide (CTAB)-capped fluorescent polymethylmethacrylate (PMMA) nanoparticles. B–D) SEM images of the PMMA nanoparticles that were obtained when different CTAB concentration in the aqueous phase has been used: B) 1×10^{-3} M, C) 0.01×10^{-3} M, and D) 0.001×10^{-3} M. E) Fluorescence spectrum of the Nile red-embedded PMMA nanoparticles obtained by dissolving 0.2 mg Nile red dye in 3 mL of monomer phase solution during nanoparticles synthesis. F) Size tunability of the PMMA nanoparticles during the application of CTAB and sodium dodecyl sulfate (SDS) surfactant with different concentrations in the aqueous phase. G) Cartoons of the shape-tuned fluorescent PMMA nanoparticles. Reproduced with permission.^[35] Copyright 2016, De Gruyter.

the polymerization temperature. Because of their lipophilic behavior, organic dye (the Nile red) molecules may randomly be dispersed inside the polymer matrix (hydrophobic) which is covered by amphiphilic CTAB molecules. CTAB-covered PMMA nanoparticles dispersed well in the aqueous phase during and after the completion of polymerization. Different parameters such as flow rates and flow rate ratios can be used for controlling the size of the polymer nanoparticles, but a dominating factor for controlling the size of the nanoparticles is surfactant concentration.^[140–141] The scanning electron microscopy (SEM) images of the obtained fluorescent PMMA nanoparticles are shown in Figure 3B–D. Spherical PMMA nanoparticles of about 70 nm diameter have resulted from 1×10^{-3} M CTAB

concentration in the aqueous phase.^[35] Similarly, 160 and 240 nm-sized PMMA nanoparticles were obtained when CTAB concentration was 10×10^{-6} and 1×10^{-6} M in the aqueous phase, respectively. Nile red molecules can be dispersed well in the hydrophobic PMMA network as nanoparticles appeared as homogeneous red-colored after repeated washing steps.^[35] The fluorescence emission peak of the Nile-red-embedding fluorescent PMMA nanoparticles is observed at 593 nm (Figure 3E). Surface properties (surface functional group or surface charge) of the polymer nanoparticles can be tuned upon the requirement for various applications. Similar to CTAB capped cationic PMMA nanoparticles, anionic PMMA nanoparticles of tunable size can be obtained by using an anionic surfactant as sodium

dodecyl sulfate (SDS), for example, in the aqueous phase (Figure 3F). In general, smaller polymer nanoparticles were obtained by the application of higher surfactant concentrations. Advantageously, small reaction volume and efficient reactant mixing ability can be realized by microflow reaction, and hence nanoparticle populations with low polydispersity were obtained which show an efficient uptake of the organic dye Nile red inside the hydrophobic PMMA network.

Similar to the Nile red dye, which was chosen here as a model dye, other classes of dyes can also be encapsulated in polymer particles.^[15,22,142] Specific types of dyes can be selected based on their color and excitation/emission wavelength. For example, rhodamine, cyanine, and BODIPY derivatives are commonly utilizing for various applications based on fluorescent nanomaterials. Derivatives of cyanine dyes are available in a wide spectrum of emission wavelengths, but their rapid degradation can be a concern. The encapsulation of cyanine dyes inside the polymer matrix is very efficient for fluorescence-based applications ranging from marker to Förster resonance energy transfer (FRET).^[143–145] Similarly, ultrabright fluorescent polymer nanoparticles can be prepared by using rhodamine and BODIPY fluorophores.^[146–148] Overall, specific types of dyes or their combinations can be incorporated during the formation of spherical fluorescent polymer nanoparticles of tunable sizes.

While spherical nanoparticles are widely utilized for various purposes, their nonspherical counterparts are extremely promising for certain specific applications such as receptor-mediated endocytosis and phagocytosis owing to their structural curvature and high surface area at the same size.^[149–151] However, it is challenging to obtain such nonspherical polymer nanoparticles in one-step because of the amorphousness of the polymeric materials. Also, it is required to perform the synthesis in one-step for incorporating the freely dispersed dye inside the polymer nanoparticle's interior. In this regard, the polyelectrolyte-supported approach can solve such concern of single-step formation of nonspherical polymer nanoparticles by initiating in situ assemblies of growing nanoparticles during the ongoing polymerization.^[102–103,136,152] Consequently, various shaped polymer nanoparticles such as ellipsoidal, dumbbell, branched, and flower shapes can be obtained (Figure 3G) in which dye can be dispersed in the same way of formation of spherical nanoparticles.

4.2. Covalently Linked Dye-Doped Fluorescent Polymer Nanoparticles

As described in Subsection 4.1 that freely-dispersed (noncovalently linked) dye-doped polymer nanoparticles are easy to prepare, with a high loading of dye content, and produced in a wide spectrum of color and emission range. Despite their efficiency, some issues can be realized in various chemical environments that may reduce quantum yield and fluorescence outcome. Two of those major concerns are: i) aggregation-caused fluorescence quenching can be realized as multiple dye molecules are encapsulated freely in the polymer matrix and ii) dye leaking may occur in the compatible solvent surroundings of the polymer particles. From the primary point of view, a

concern of aggregation-caused quenching can be overcome by the implementation of nanomaterials that show the characteristics of aggregation-induced emission. The fluorogens that show aggregation-induced emission are advantageous in many ways because they exhibit superior photostability, brightness, and high quantum yield.^[130,153] For obtaining the photostable fluorescent polymer particles, functionalized polymers tailored with aggregation-induced emission functions can be used.^[154] Usually, in the dye-doped polymer particles, organic dyes encapsulate into the organic nanoparticles. Organic dyes contain plenty of aromatic rings and hence they are flat molecules that tend to stack or aggregate. The introduction of a bulky hydrophobic counter-ion as a spacer between charged dyes can be able to prevent such aggregation-caused quenching.^[52,155] Similarly, the comparative study can also be carried out by tailoring bulky side groups to control the aggregation of fluorophores in the polymer matrix.^[146,156–157]

If fluorescent dyes can be linked with a polymer network via covalent bonding, then those concerns of leaking and aggregation-caused quenching can be overcome effectively. Therefore, here a model synthesis approach of the covalently-linked fluorophore with polymeric nanoparticle network is provided.^[135] In this strategy, the fluorophore unit has been linked covalently with MMA monomer prior to initiating the polymerization process. In this way, the monomer itself becomes fluorescence-active, and hence the nanoparticles too after completion of polymerization. In general, a wide range of different fluorescent monomers can be synthesized by covalently linking various fluorophores with simple monomers such as MMA or styrene. Here, a synthesis procedure of 5-methyl-2-(pyridine-2-yl)thiazol-4-yl methacrylate (fluorescent MMA or FL-MMA) is shown (Figure 4A). Briefly, FL-MMA can be prepared by linking 5-methyl-2-(pyridine-2-yl)thiazol-4-ol (synthesized from picolinonitrile and 2-mercaptopropanoic acid precursor) with pure MMA. Once FL-MMA is ready to use, their polymerization can be initiated. FL-MMA is a solid compound that can be dissolved in pure MMA liquid for polymerization. In a model synthesis, 5% FL-MMA was dissolved in MMA for proceeding with the polymerization process as shown in Figure 4B. Anionic surfactant SDS can control the size and surface charge of polymer nanoparticles. Around 240 nm-sized fluorescent PMMA nanoparticles were obtained when 10×10^{-6} M SDS was used in the aqueous phase (Figure 4C).^[135] Fluorescence emission of the obtained fluorescent PMMA nanoparticles has appeared at 411 nm (Figure 4D). By using different types of surfactants and various fluorophores of different emission wavelengths, covalently linked fluorescent polymer nanoparticles of tunable interior and surface properties can be prepared. The use of photostable and chemically stable fluorescent polymer nanoparticles can support the sustained fluorescence yield hence useful in cellular markers or probes.

4.3. Fluorescent Dye at Surface of Polymer Nanoparticles

Soft polymer nanoparticles become fluorescence-active by the presence of fluorophores inside the matrix (interior) or at the surface. As shown in Subsections 4.1 and 4.2 that fluorophores inside the matrix can be incorporated noncovalently

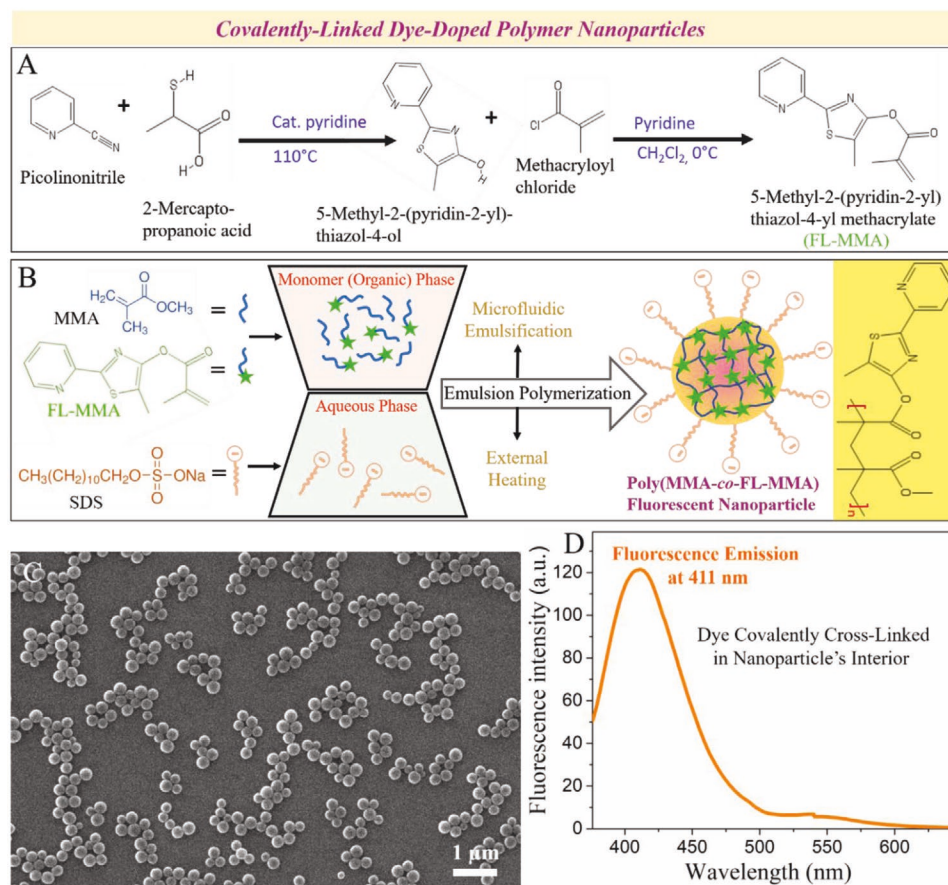


Figure 4. Covalently linked dye-doped fluorescent polymer nanoparticles. A) Chemical synthesis of the fluorescent derivative of the methylmethacrylate (MMA) monomer, i.e., 5-methyl-2-(pyridin-2-yl)thiazol-4-yl methacrylate (FL-MMA). B) Synthesis ingredients of the covalent cross-linked dye-doped PMMA nanoparticles. C,D) SEM image and fluorescence spectrum of the fluorescent PMMA nanoparticles obtained by using 5:95 FL-MMA:MMA weight ratio in the monomer phase and 0.01×10^{-3} M SDS in the aqueous phase, respectively. Reproduced with permission.^[35] Copyright 2016, De Gruyter.

or covalently to make the polymer nanoparticle fluorescence active. Besides the interior, here, a strategy has been applied where fluorescent dye (fluorophore) can be attached to the surface of nanoparticles. In general, the surface energy of the nanoscale particles is high,^[158] and hence irregular aggregation can be initiated if the surface is not properly protected. Usually, amphiphilic surfactant or polyelectrolytes can potentially be used as an interfacial agent for capping the surface of nanoparticles in the solution and helps to avoid their uncontrolled aggregation.^[102] The molecules attached at the surface of nanoparticles do not only protect the nanoparticles from uncontrolled aggregation but also useful in initiating the specific interfacial interactions with targeted objects such as cell surface or other types of nanoparticles.^[159] Furthermore, the application of biocompatible polymers such as amphiphilic block copolymer of polyethylene glycol or other polymers at the surface can enhance the bio-interactions. If interfacial agents possess the fluorescence function along with amphiphilicity, then they can support the formation of polymer nanoparticles of tunable size, surface charge, and fluorescence intensity in a single step. Here, a water-soluble disodium 2,2'-[(1E)-triazole-1,3-diyl]bis(6-methyl-1,3-benzothiazole-7-sulfonate) (Titan yellow) dye has been used which can

mimic the role of the interfacial agent during the synthesis of PMMA nanoparticles.^[35] The organic monomer phase is composed of MMA, EGDMA, and AIBN whereas various concentrations of Titan yellow have been applied in the aqueous phase (Figure 5A). Smaller-sized nanoparticles were obtained by using a high concentration of Titan yellow in the aqueous phase. Also, fluorescent nanoparticles obtained here show the fluorescence spectral peak at 425 nm (Figure 5B). Similarly, a wide range of various fluorescence-active interfacial agents can be used during the formation of single-step fluorescent polymer nanoparticles.

4.4. Fluorescent Dye Labeled Surface-Network through Bioconjugation

For bioorthogonal labeling, fluorescent monoclonal antibodies are popular choices.^[160–162] The suitable fluorescent dye can be coupled to various proteins including antibodies, streptavidin, and avidin. In this regard, monoclonal antibodies labeled with near-infrared fluorophores have potential use in disease detection.^[68] With this motivation, here, a model reaction strategy for dye-labeled streptavidin linked to a biotinylated molecular

network on the surface of polymer nanoparticles through bioconjugation has been performed. Applying biomolecules on the surface of polymer nanoparticles not only improves biocompatibility but also promotes efficient interaction based on affinity such as biotin-streptavidin interaction.^[163] As shown in Figure 5C, initially, CTAB-covered PMMA nanoparticles (zeta potential +20 mV) were synthesized via a semi-microfluidic process.^[35] The cationic surface of nanoparticles is suitable to bind anionic molecules/macromolecules through electrostatic interaction. Therefore, anionic poly-L-glutamic acid (PGA) and cationic poly-L-lysine (PLL) was subsequently applied electrostatically to the CTAB-covered cationic PMMA nanoparticles. PGA and PLL are biopolymers (polypeptides) and they have a strong ability to assemble in multilayers through electrostatic interaction.^[164] With PGA and PLL, therefore, the desired number of layers can be applied through the layer-by-layer assembly. After successful PGA-PLL assembly on the surface of nanoparticles, the primary amine group at the outer surface of PLL can potentially initiate the interaction to bind with biotin molecules as shown in Figure 5C.^[165] Biotin is a naturally occurring vitamin that binds with high affinity to proteins such as streptavidin and avidin without altering their biological activities.^[163,166–167] N-Hydroxysuccinimide (NHS)-activated biotins react efficiently with primary amino groups to form stable amide bonds. For a model reaction, here, a Sulfo-NHS-LC-LC-Biotin (sulfosuccinimidyl-6-[biotinamido]-6-hexanamide hexanoate) has been used to bind with the primary amine of PLL. The spacer length of the biotin can be chosen in dependence on the requirements during applications, on the one side. On the other side, biotin has a very strong affinity to conjugate with streptavidin.^[163] Here, we have selected a fluorescent dye-labeled streptavidin for the interaction with biotin. Alexa Fluor 594 dye (used here) is a bright (red fluorescent dye) and is excited at 594 nm wavelength.^[35] Polymer nanoparticles after PGA-PLL and biotin-streptavidin conjugation become fluorescence-active and show a fluorescence spectral peak at 619 nm as shown in Figure 5D. An SEM image of the PMMA nanoparticles after dye-labeled streptavidin conjugation is shown in Figure 5E. Similarly, other types of proteins or nucleic acid-functionalized fluorescent nanoparticles can be developed for biosensing applications. For instance, dye-loaded polymer nanoparticles were developed for target recognition by surface functionalization with DNA that functions based on the donor-acceptor Förster Resonance Energy Transfer.^[168]

5. Fluorescent Polymer Microparticles

As shown in Section 4, various fluorescent dyes can be linked to the polymeric network of the nanoscale polymer particles noncovalently or covalently in the interior and at the immediate surface as an interfacial agent or through layer-by-layer surface conjugation. For nanoscale polymer particles, a semi-microfluidic emulsion polymerization approach has been applied.^[35] This section reviews the synthesis techniques of hydrophobic and hydrophilic microscale fluorescent polymer particles that have been performed via photopolymerization. Mainly, the size tunability of generated particles by flow rates, flow rate ratios, surfactant concentration, and microflow channel dimension has

been described. Also, a computer-controlled flow rate program has been applied for systematic color combinations in polymer microparticles. It is shown that droplet microfluidics^[169–171] is very promising for simultaneous size and color tunability in a wide variety. Considering the wetting properties (surface interaction based on hydrophilicity and hydrophobicity) of polymer particles, a surface-functionalized technique for microreactor chips is also briefly explained.

5.1. Hydrophobic Polymer Microparticles

The availability of a wide spectrum of various organic monomers allows the formation of a diverse range of hydrophobic polymer particles. Here, a basic synthesis of the multicolored dye-doped poly(tripropylene glycol diacrylate) (PTPGDA) hydrophobic fluorescent microparticles has been described. Crossflow microfluidic setup^[120] as shown in Figure 2B is very suitable to generate the droplets of uniform size and, therefore, the polymer microparticles. The slug (droplet) of the hydrophobic monomer phase in the flowing aqueous phase can be photopolymerized to form hydrophobic microparticles.^[42] The surface of the silicon chip inside the microreactor is hydrophilic that is compatible with the aqueous carrier phase.^[121] The monomer phase is made up of the tripropylene glycol diacrylate (TPGDA) monomer and 2-hydroxy-2-methylpropiophenone (HMPP) photoinitiator along with various organic dyes (Figure 6A). Various hydrophobic cross-linker can also be added for controlling the interior and surface properties such as porosity of polymer particles.^[66] Droplets of the monomer phase can be generated in the shear force of the aqueous carrier phase.^[115] Problems with interfacial instability can arise when the two immiscible phase meets at the T-junction of the microreactor.^[116,120] The surface tension can be reduced and interfaces can be stabilized by the addition of an amphiphilic surfactant in the aqueous carrier phase.^[139] Here, the anionic surfactant SDS has been used in the aqueous carrier phase. The presence of SDS is not only reducing the surface tension of the droplets but is also able to control the particles' size at various concentrations.^[42] The generated droplets of the monomer phase are flowing in the FEP transparent tubing and polymerized immediately upon irradiation of UV light arranged in the setup (Figure 2B). PTPGDA microparticles of size range between 50 and 150×10^{-6} m were obtained by the application of SDS concentration between 2×10^{-3} and 5×10^{-3} M along with various flow rate ratios of carrier phase to monomer phase (Figure 6B–E).^[42] Similar to SDS, other surfactants can also be used in an aqueous phase such as CTAB for tuning the size and surface charge of polymer particles. Also, other types of carrier solution such as silicon oil, Novec 7500, or perfluoromethyldecalin (PP9) immiscible to monomer phase can be applied for tuning microparticles diameter in a broad size spectrum. During the synthesis of microparticles, various types of individual dye or a combination of various dyes can be dissolved in the monomer phase to make the generated microparticles fluorescence active. Here, two types of synthesis were performed: The first type of particles where only one fluorescent dye (Nile red) has been dissolved in the monomer phase. In this case, the obtained fluorescent microparticles show the fluorescence spectral peak at 620 nm

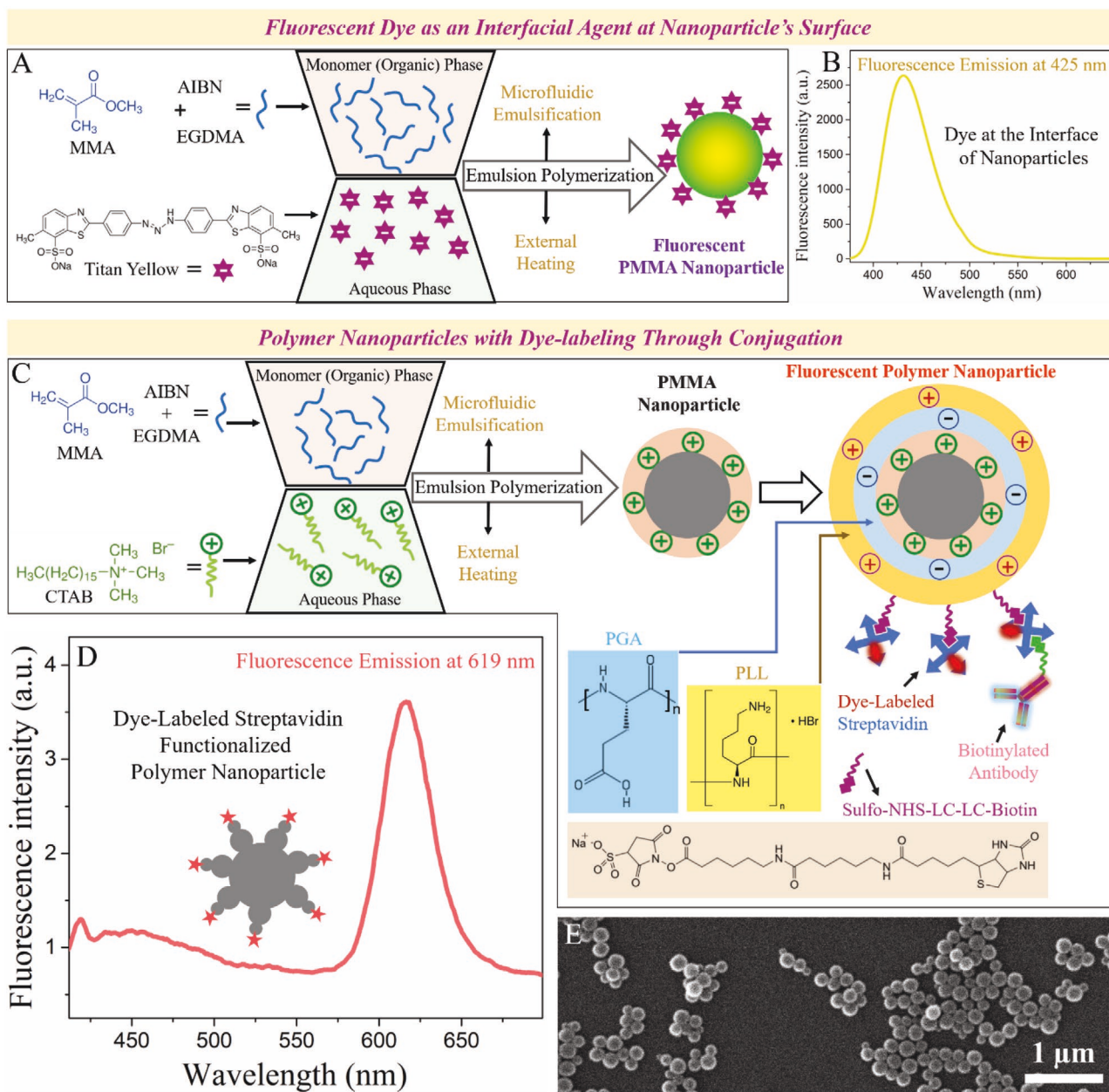


Figure 5. Fluorescent dye at the interface of polymer nanoparticles. A) Disodium 2,2'-[(1E)-triaz-1-ene-1,3-diyl]bis(6-methyl-1,3-benzothiazole-7-sulfonate) (Titan yellow), a water-soluble fluorescent dye, also acts as an interfacial agent during the PMMA nanoparticles synthesis that controls the size and surface charge of nanoparticles together with their fluorescence activeness. B) Fluorescence spectrum of the Titan yellow-covered PMMA nanoparticles. C) Synthesis scheme for the layer-by-layer conjugation of polypeptides, biotin, and fluorescent-labeled streptavidin that form the fluorescent polymer nanoparticles. D,E) Fluorescence spectrum and SEM image of the layer-by-layer conjugated fluorescent PMMA nanoparticles, respectively. Reproduced with permission.^[35] Copyright 2016, De Gruyter.

(Figure 6F). The second type of fluorescent polymer particles in which two different dyes with 60:40 ratio (Nile red:12-(7-nitrobenzofuran-4-ylamino)dodecanoic acid (NBD)) were dissolved and two spectral peaks (532 and 620 nm) in the fluorescence spectrum have been realized (Figure 6F). The tunable surface porosity in PTPGDA microparticles can be generated by applying a relatively high flow rate of the monomer phase (Figure 6G).^[42,66] Overall, here, the microfluidic synthesis techniques for obtaining systematically tunable size and color of

microparticles has been provided. The colored and hydrophobic fluorescent PTPGDA microparticles can potentially be applied for the labeling of various materials systems.

5.2. Hydrophilic Polymer Microparticles

Hydrophilic polymer particles are an important class of polymeric materials due to their structural and interfacial

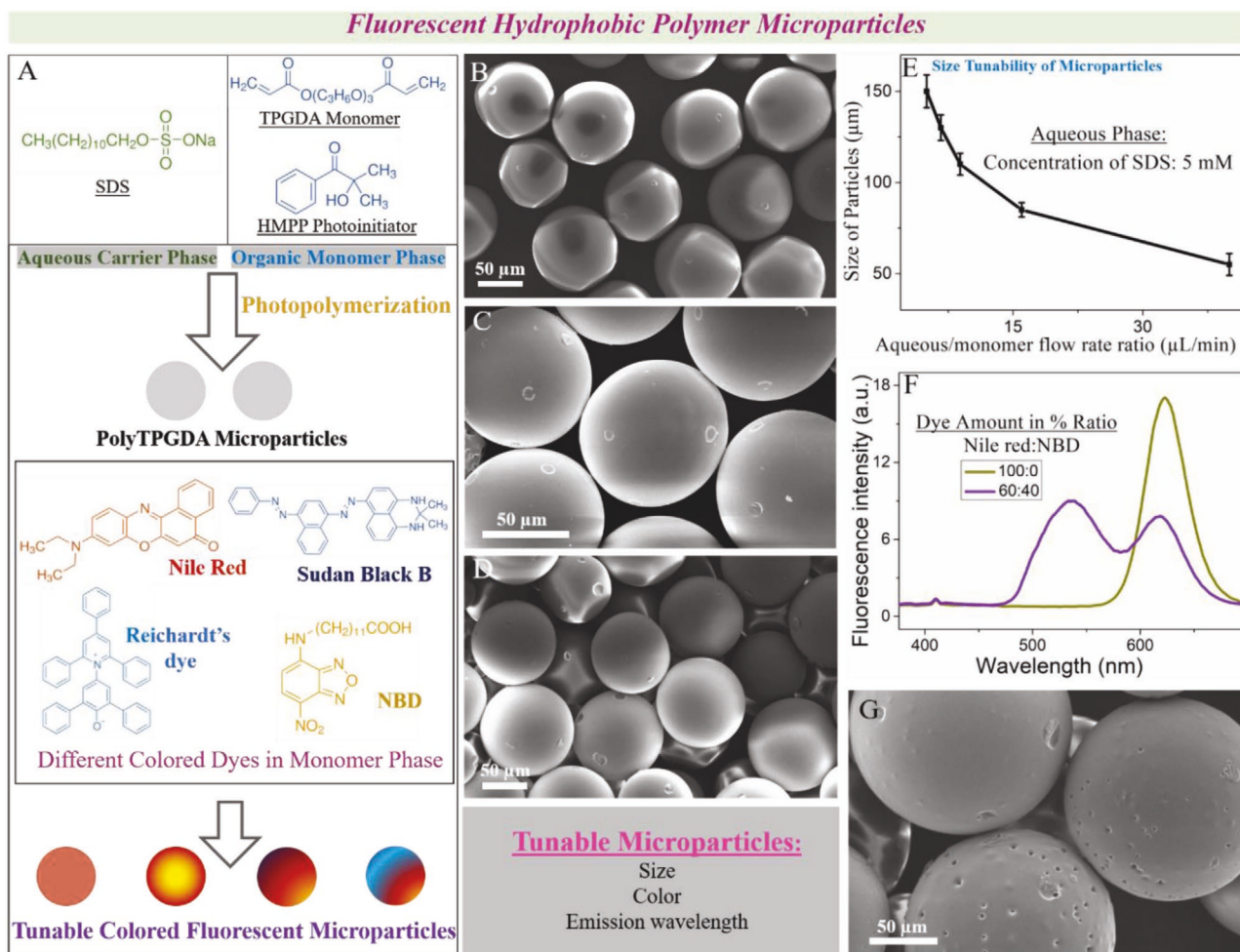


Figure 6. Microscale hydrophobic fluorescent polymer particles. A) A synthesis scheme for the formation of fluorescent poly(tripropylene glycol diacrylate) (PTPGDA) microparticles by incorporating various combinations of organic dyes. B–D) SEM images of the PTPGDA microparticles synthesized at different reaction conditions: B) SDS concentration in the aqueous phase is 5×10^{-3} M and aqueous to monomer flow rate ratio is 400/10 $\mu\text{L min}^{-1}$, C) SDS concentration in the aqueous phase is 2×10^{-3} M and aqueous to monomer flow rate ratio is 400/10 $\mu\text{L min}^{-1}$, and D) SDS concentration in the aqueous phase is 2×10^{-3} M and aqueous to monomer flow rate ratio is 400/25 $\mu\text{L min}^{-1}$. E) Graphical results of the size of microparticles obtained at various flow rate ratios of aqueous to monomer phase. F) Fluorescence spectra of the two different dyes, Nile red and NBD, embedded in various concentration ratios in the microparticles during the microfluidic synthesis. G) SEM image of the porous PTPGDA microparticles obtained when 2×10^{-3} M SDS is used in the aqueous phase and flow rate ratio of aqueous to monomer phase was 400/45 $\mu\text{L min}^{-1}$. Reproduced with permission.^[42] Copyright 2015, Royal Society of Chemistry.

characteristics and functions. Accumulation of water in the polymeric network makes them gel-like materials that swell and deswell, creates pores and wrinkles, and carry a variety of functional components in their network.^[172] Therefore, these particles as hydrogel materials are extremely useful for a wide range of various biomedical applications such as scaffolds for tissue engineering and carriers for drug delivery.^[173] The amount of water in the microparticles can be controlled during synthesis.^[174] Polyacrylamide, polyethyleneglycol (PEG), polylactic-co-glycolic acid (PLGA) like hydrophilic polymeric networks are biocompatible and biodegradable.^[175] Biocompatible hydrogel particles can become fluorescence-active by the incorporation of fluorophores inside the particles.^[176] Here, the synthesis strategy for the size and color-tunable fluorescent polyacrylamide microparticles through photopolymerization in a droplet microfluidic setup is described (Figure 7). For

hydrogel particles, generated droplets are of the aqueous phase. The aqueous phase is made up of the acrylamide monomer, bisacrylamide cross-linker, 2-hydroxy-2-methylpropiophenone photoinitiator (in ethylene glycol), and various water-soluble fluorescent dyes. Immiscible to the monomer phase, the carrier phase is made up of the Novec 7500 and picosurf (surfactant) (Figure 7A).^[176] A silicon chip has been embedded in the microreactor chamber for releasing the monomer phase droplets.^[65] Originally, the surface of the silicon chip is hydrophilic. Therefore, its surface has been functionalized with trichloro(1*H*,1*H*,2*H*,2*H*-perfluorooctyl)silane to make it compatible with the carrier phase and supporting the generation of droplets of the aqueous monomer phase (Figure 7C). The size of polyacrylamide microparticles can be systematically tuned by changing the flow rates, flow rate ratios, picosurf concentration in the carrier phase, and microchannel diameter.^[65,176]

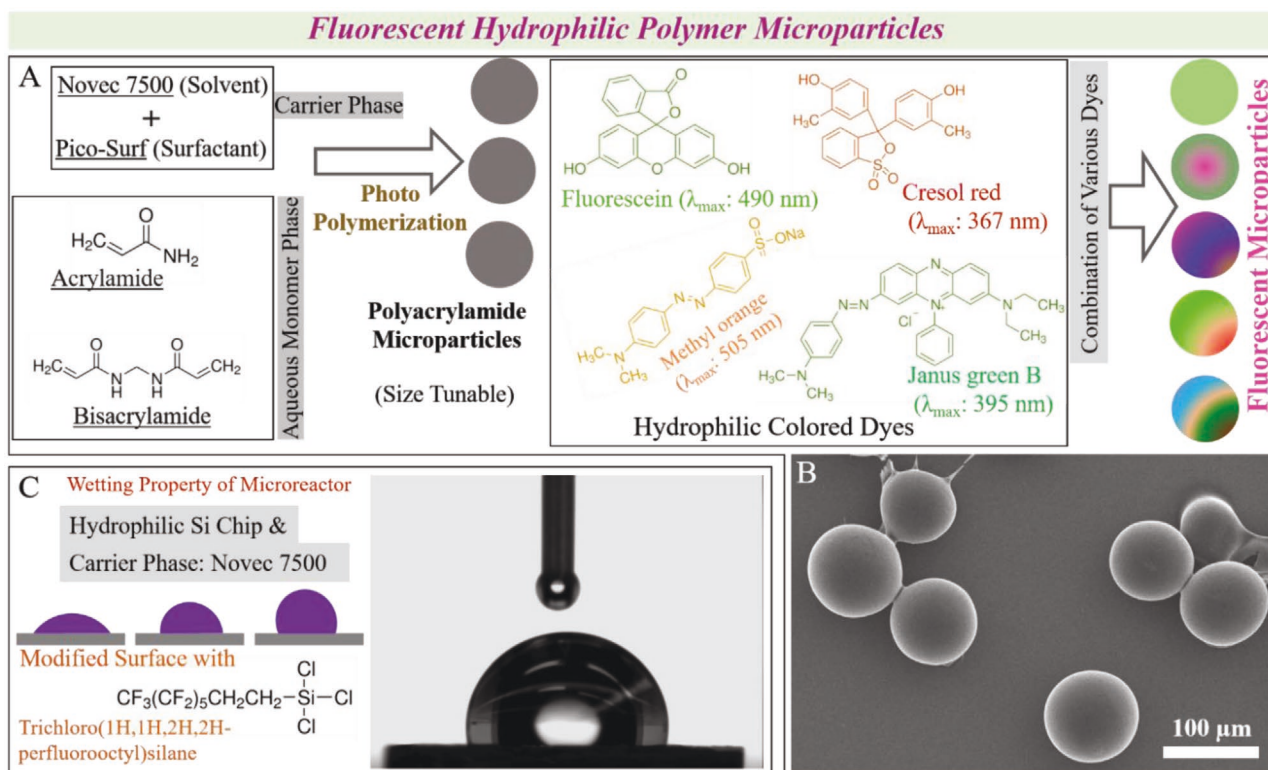


Figure 7. Hydrophilic polyacrylamide fluorescent microparticles. A) Synthesis scheme for the generation of tunable-sized multicolored polyacrylamide microparticles. B) SEM image of the polyacrylamide microparticles obtained when carrier to monomer phase flow rate ratio was 200/30 $\mu\text{L min}^{-1}$ in which 1 mL 0.5% picosurf was dissolved in 5 mL of pure Novec 7500 in carrier phase. C) Surface functionalization scheme of the silicon chip that embedded in the microreactor for the compatibility of the carrier phase. Contact angle image of the water drop deposited on the functionalized silicon chip surface. Reproduced with permission.^[65] Copyright 2015, American Chemical Society.

A representative SEM image of the polyacrylamide microparticles of about 100 μm diameter has been shown in Figure 7B which was obtained at the flow rate ratio of 200/30 $\mu\text{L min}^{-1}$ carrier/monomer phase.^[65] Similarly, the size of the polyacrylamide microparticles can be controlled precisely between 30 and 800 μm by application of various flow rate ratio and surfactant concentration.^[65]

5.3. Color Tunability and Fluorescence Imaging of Polymer Microparticles

Hydrophobic PTPGDA microparticles (Subsection 5.1) and hydrophilic polyacrylamide microparticles (Subsection 5.2) can become fluorescence-active by incorporation of fluorescent dyes of various colors and emission wavelengths (Figure 8). A computer-controlled syringe pump-supported microflow setup is useful to mix various dyes in a controlled amount with their color combination. Continuous circulation of droplets of the monomer phase in the flow of carrier liquid can efficiently mix various dyes in droplets with uniform distribution.^[42] Figure 8A shows an overview of the colored microparticles. A single type of dye was dissolved in the monomer phase, hence monochromatic polymer particles were obtained. Here, NBD dye-doped PTPGDA microparticles were obtained through photopolymerization in droplet microfluidics.^[42] A darkfield image and a fluorescence

image with an excitation wavelength range of 450–490 nm of NBD-doped PTPGDA microparticles were captured through a fluorescence microscope as shown in Figure 8B,C. Similar to NBD, a wide range of various organic dyes (such as Nile red, etc.) of different emission wavelengths and colors depending on desired labeling applications can be introduced in the polymer microparticles during synthesis. Different types of individual colored monochromatic microparticles can be mixed on one spot for imaging, and also can be used similarly during multilabeling of materials systems. Likewise, various dyes can be mixed in a single particle and its fluorescence image can be captured at different excitation wavelengths. As a model mix-colored system, here two different types of monochromatic particles (NBD-doped green and Nile red-doped pink) and one type of bicolored microparticles (a mixture of the Nile red and NBD dye in a single-particle) were deposited on a single spot for fluorescence imaging (Figure 8D). Nile red-embedded particles show bright fluorescence at higher excitation wavelength whereas NBD-embedded particles at relatively shorter ones. Therefore, the same spot of mix-colored particles (Figure 8D) has been excited at two different wavelengths: 510–560 nm excitation wavelength (Figure 8E) and 450–490 nm excitation wavelength (Figure 8F). Similarly, many types of color combinations can be tuned in hydrophobic fluorescent polymer microparticles.

While organic dyes can be incorporated in hydrophobic microparticles, a broad spectrum of colored hydrophilic

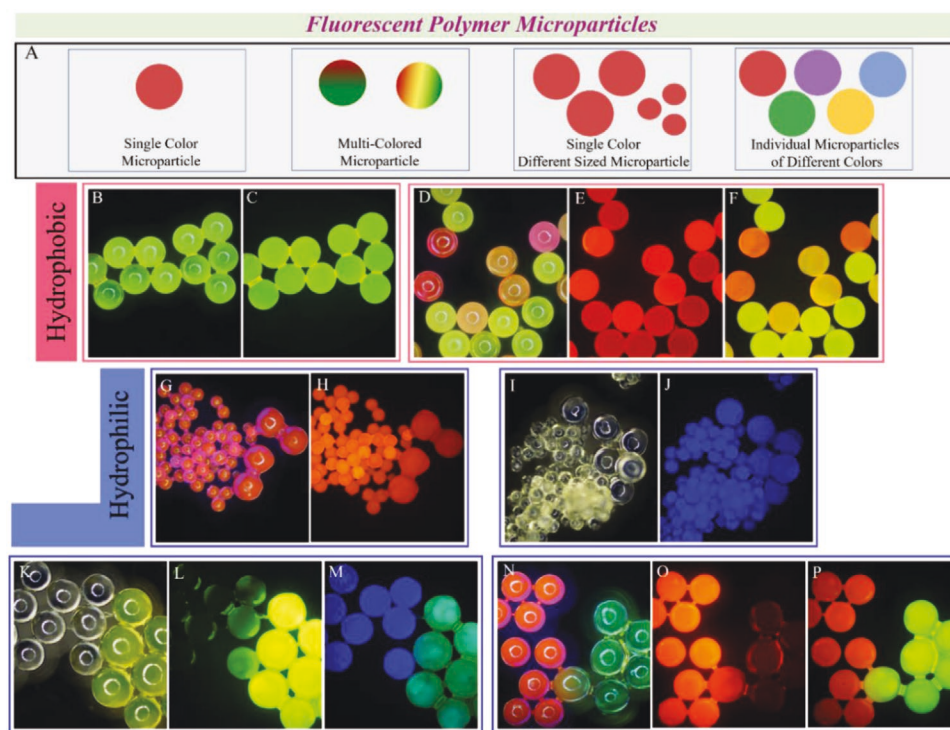


Figure 8. Fluorescence microscopy images of the hydrophobic and hydrophilic fluorescent polymer microparticles. A) A scheme for the polymer particles of multiscale and multicolors. B–F) Hydrophobic poly(tripropylene glycol diacrylate) (PTPGDA) fluorescent microparticles: B) Darkfield image of the 12-(7-nitrobenzofuran-4-ylamino)dodecanoic acid (NBD) dye-doped PTPGDA microparticles and C) their fluorescence image captured at excitation wavelength range 450–490 nm. D) Darkfield image of three different colored particles, Nile red embedded pink, NBD embedded green, and 50:50 mixture of Nile red:NBD embedded orange. E, F) are the fluorescence images of the same sample at different excitation wavelengths: E) excited at 510–560 nm and F) 450–490 nm. G–P) Hydrophilic polyacrylamide fluorescent microparticles: G) Darkfield image of the Orange G dye-doped polyacrylamide microparticles of two different sizes and H) their fluorescence image captured at excitation wavelength range 510–560 nm. I) Darkfield image of the Titan yellow dye-doped polyacrylamide microparticles of two different sizes and J) their fluorescence image captured at excitation wavelength range 300–390 nm. K) Darkfield image of the two different colored polyacrylamide microparticles, Titan yellow contained dark blue particles and fluorescein contained green particles. L, M) Their fluorescence images captured at the excitation wavelength range 450–490 and 300–390 nm, respectively. N) Darkfield image of the two different colored polyacrylamide microparticles, Orange G contained pink particles and fluorescein contained green particles. O, P) Their fluorescence images captured at excitation wavelength range 510–560 and 450–490 nm, respectively. B–F) Reproduced with permission.^[42] Copyright 2015, Royal Society of Chemistry. G–P) Reproduced with permission.^[176] Copyright 2016, Elsevier Ltd.

polymer microparticles can be obtained by similarly introducing water-soluble fluorescent dyes.^[176] For microscale particles, microfluidics is very promising for color and size tuning very precisely. Here, fluorescence imaging of the fluorescent polyacrylamide microparticles of different color and size are shown. As shown in Figure 8G, two different-sized Orange G dye-doped polyacrylamide microparticles were displayed (darkfield image) which reveal bright fluorescence at excitation wavelength range 510–560 nm (Figure 8H). Similarly, Titan yellow-doped polyacrylamide microparticles of two different sizes were displayed in Figure 8I (darkfield image) and Figure 8J (fluorescence image with excitation wavelength 300–390 nm). Similar to two-different sized monochromatic microparticles, particles of different colors can be deposited on a single spot for fluorescence imaging, and hence can also be used for the multilabeling purpose of various materials systems. As shown in Figure 8K, two different colored microparticles (Titan yellow-doped blue colored and fluorescein-doped yellowish green colored) were deposited on a glass slide and their darkfield image was obtained through an optical microscope. The same spot has been excited at two different wavelengths in a fluorescence

microscope, fluorescein-doped microparticles show bright fluorescence at 450–490 nm excitation wavelength (Figure 8L) and Titan yellow-doped microparticles show fluorescence at 300–390 nm (Figure 8M). Similarly, orange G-doped microparticles and fluorescein-doped microparticles were deposited on a single spot (Figure 8N) and their fluorescence images have been captured at two different excitation wavelength 510–560 (Figure 8O) and 450–490 nm (Figure 8P), respectively.

6. Multiscale Assemblies of Fluorescent Polymer Particles

Fluorophore linking to polymeric particles in terms of various color combinations and tunable size of particles at nanoscale and microscale has been described in Sections 4 and 5. In this section, experimental results of assemblies of size-tuned and color-tuned fluorescent polymer particles are summarized and reviewed. The properties of individual polymer particles such as swellability, pH responsiveness, degradability, mechanical strength, and surface functionality can be controlled before

initiating the assemblies.^[48] A novel type of hybrid polymeric particles can be generated that reveal coupled properties when two different types of polymer particles can be assembled. If the distance between assembling fluorescent particles can be controlled within the range of Förster radius, then fluorescent assembly particles can allow the occurrence of donor-acceptor-based energy transfer process through distance-dependent Förster resonance energy transfer (FRET).^[177–179] Assemblies of the nanoscale fluorescent polymer particles are displayed in the first part whereas nano-micro assembly of fluorescent polymer nanoparticles and microparticles is provided in the latter part.

6.1. In Situ Assembly of Fluorescent Polymer Nanoscale Particles

Two different types of dye-doped fluorescent polymer nanoparticles can assemble through the interface and form assembly nanoparticles. Initially, one type of fluorescent polymer nanoparticle was synthesized via semi-microfluidic synthesis (pre-formed nanoparticles).^[103,136,176] Subsequently, the formation and in situ assembling of the second type of polymer nanoparticles can be initiated through emulsion polymerization.^[67] The surface of pre-formed nanoparticles has been tailored as swellable and cationic surface charged for potentially interact and entrap the incoming nanoparticles of opposite surface charge for assemblies.^[159] Instead of molecular surfactant, a water-soluble ionic monomer can be used as an interfacial agent that protects the surface of nanoparticles against uncontrolled aggregation between the same types of nanoparticles. Simultaneously, the charged interfacial monomer can also initiate the formation of a polymeric network at the surface of core polymer nanoparticles. Hence, at the end of the polymerization process, core-shell type co-polymer nanoparticles can be obtained in which the surface polymeric network is hydrophilic that swells in the aqueous solution, and a core polymeric network is hydrophobic.^[159] As shown in **Figure 9A**, the carrier aqueous phase is made up of the water-soluble monomer diallyldimethylammonium chloride (DADMAC) and the dispersed organic phase is made up of the MMA monomer, EGDMA cross-linker, AIBN initiator, and organic fluorescent dye Prodan (*N,N*-Dimethyl-6-propionyl-2-naphthylamine).^[67] Emulsification of both immiscible phases was performed in a cross-flow microreactor (**Figure 2A**) and further polymerization has been proceeded externally at polymerizing temperature. After completion of the polymerization process, soft and swellable surface-layered (poly-DADMAC) Prodan-doped PMMA nanoparticles were obtained.^[67,159] After cleaning through repeated washing steps, these Prodan-doped PMMA nanoparticles (pre-formed nanoparticles—host) were taken into a reaction tube in which an emulsion solution of the second type of polymer nanoparticles (guest) has been inserted and further polymerization process initiated. The aqueous carrier phase of the guest nanoparticles was made up of the anionic surfactant sodium dodecyl sulfate (SDS) and the dispersed organic phase contained MMA, EGDMA, AIBN, and organic dye Nile red.^[67] The surface of host nanoparticles is cationic where anionic guest nanoparticles can systematically assemble via electrostatic interaction. The concentration of SDS in the aqueous phase

has been varied for tuning the size of the assembling guest nanoparticles (**Figure 9B,C**). Prodan-doped host PMMA nanoparticles reveal a fluorescence peak at 435 nm whereas Nile red-doped PMMA nanoparticles show the fluorescence peak at 590 nm.^[67] After completion of assembly through polymerization process, a single spectrum shows two different peaks at 435 and 590 nm as shown in **Figure 9D**.

In general, the strategy to form a swellable layer at the surface of nanoparticles is very promising. On one hand, it creates the nanoparticles with stealth properties and, on the other hand, that allow entrapping molecular as well as smaller sized particulate functional components for various purposes. Similar to ionic monomer used in a model strategy here, other types of macromolecules can also be used to tailor the soft surface of nanoparticles. For instance, functionalized amphiphilic block copolymers have been used that can support the nanoparticles with stealth properties for the study to visualizing a single fluorescent nanoparticle.^[146] Also, systematic tailoring of the soft surface of the nanoparticles not only prevents the interparticle aggregation in an uncontrolled manner but also allows the specific target interaction such as with biological or materials systems. Various types of fluorescent polymer nanoparticles by doping different fluorophores covalently, noncovalently or by other means can be fixed into the surface polymeric layer of the core fluorescent polymer particle. In this way, a single fluorescent assembly particle can be generated with the desired number of fluorescence functions. Such tunable fluorescent assembly nanoparticles can be useful in the labeling of various materials systems.

6.2. Embedding Nanoscale Particles in Microparticles

Microfluidics is advantageous in combining various molecular and particulate components precisely in a continuous flow manner.^[180] Uniform microscale particles of tunable sizes can simply be formed by solidifying the monomer droplets by external light (photopolymerization).^[56] As explained in Subsection 6.1 that assemblies between two types of fluorescent polymer nanoparticles were realized through electrostatic interactions. Besides, the assemblies of nanoparticles and microparticles were performed and described in this subsection by incorporating smaller nanoparticles into the interior of the larger microparticles.^[176] Initially, NBD-doped fluorescent PMMA nanoparticles were synthesized via a semi-microfluidic method.^[35] The aqueous phase for the synthesis of fluorescent polymer nanoparticles was made up of anionic surfactant SDS and monomer phase with MMA, EGDMA, AIBN, and NBD dye (**Figure 9E**). Afterward, NBD-doped fluorescent nanoparticles were dispersed in the monomer phase made for the synthesis of polyacrylamide microparticles. The monomer phase for polyacrylamide microparticles, therefore, contains water, acrylamide monomer, bisacrylamide cross-linker, HMPP photoinitiator (in ethylene glycol), fluorescein dye, and NBD-doped fluorescent PMMA nanoparticles. The carrier phase is made up of Novac 7500 and picosurf (**Figure 9E**). The microfluidic photopolymerization process has been performed to obtain the NBD-doped nanoparticles embedded tunable-sized fluorescent polyacrylamide microparticles (**Figure 9F,G**). The overall size

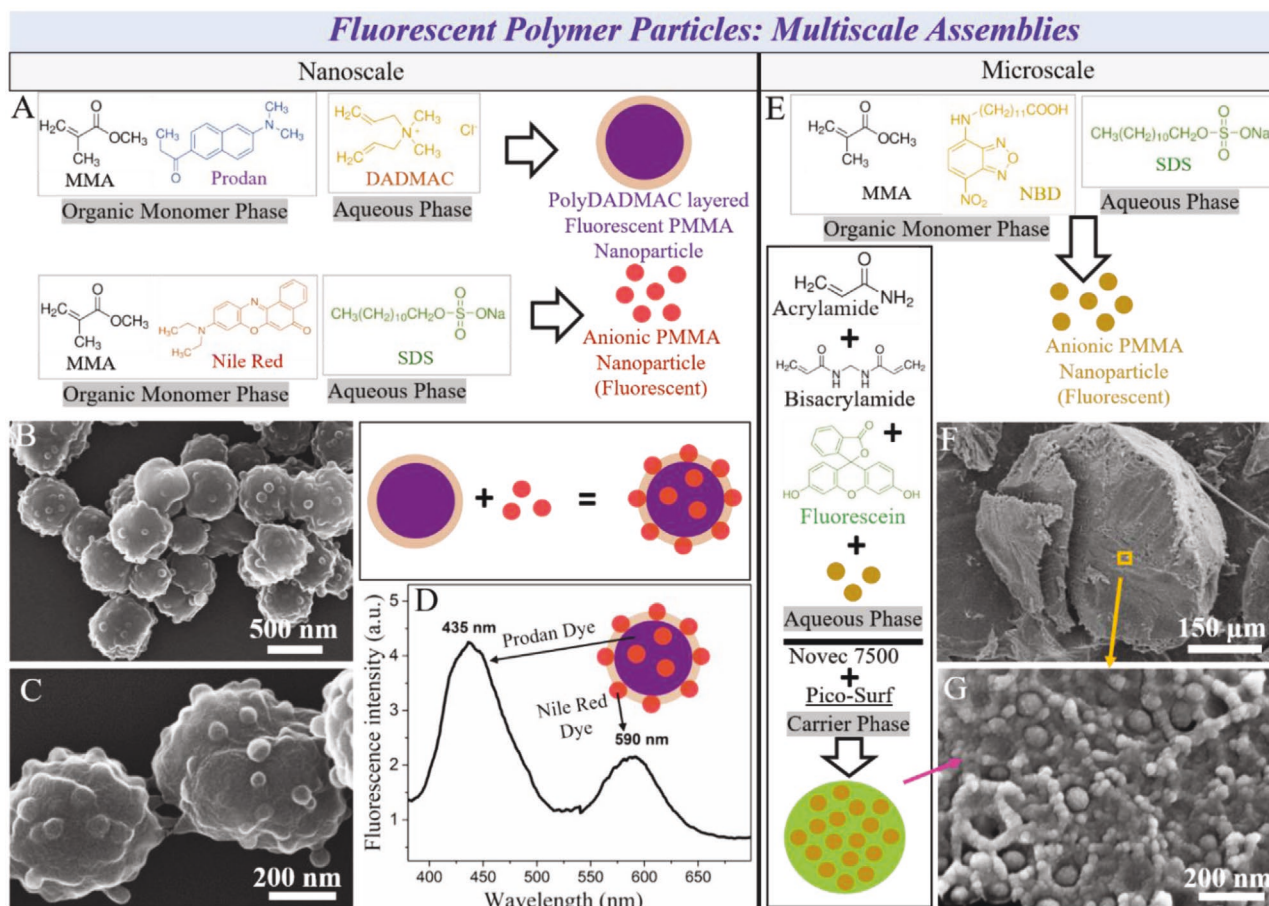


Figure 9. Multicolored assemblies of fluorescent polymer particles at multiscale levels. A) A general synthesis scheme for the generation of cationic core-shell type and anionic spherical polymethylmethacrylate (PMMA) nanoparticles. B, C) SEM images of the PMMA-PMMA nanoassembly particles obtained at different reaction conditions: B) Sodium dodecyl sulfate (SDS) covered PMMA nanoparticles formed during use of 0.01×10^{-3} M SDS in the aqueous phase and simultaneously assembled on the surface of pre-formed polydiallyldimethylammonium chloride (polyDADMAC) covered cationic PMMA nanoparticles. C) SDS-covered PMMA nanoparticles formed during the use of 0.001×10^{-3} M SDS in the aqueous phase and simultaneously assembled on the surface of pre-formed polyDADMAC covered cationic PMMA nanoparticles. D) Fluorescence spectra of the nanoparticles shown in (B) in which SDS covered assembling spherical PMMA nanoparticles contain the Nile red dye and core-shell PMMA nanoparticles contain the *N,N*-Dimethyl-6-propionyl-2-naphthylamine (Prodan) dye. E) A synthesis concept of the 12-(7-nitrobenzofuran-4-ylamino)dodecanoic acid (NBD) contained anionic spherical nanoparticles embedded in the fluorescein dye contained polyacrylamide microparticles. F, G) The lower and higher magnified SEM images of the NBD-contained PMMA nanoparticles embedded fluorescein contained polyacrylamide microparticles. A–D) Reproduced with permission.^[67] Copyright 2015, Wiley-VCH. E–G) Reproduced with permission.^[176] Copyright 2016, Elsevier Ltd.

of the polyacrylamide can systematically be tuned by microchannel diameter, flow rate ratios, and picosurf concentration in the carrier phase. The properties of the microparticles such as interior cross-linking, swellability, porosity, and surface wrinkling can be tailored depending upon the requirements during various applications ranging from tissue engineering to bio-sensing. Also, a wide range of fluorophore-functionalized size and shape-controlled fluorescent polymer nanoparticles can be incorporated inside the larger microparticles to make the fluorescent assembly microscale particles.

7. Hierarchical Labeling Concept Based on Size and Color

Whereas monochromatic fluorescent polymer particles are promising for the labeling of a particular target in the biological

as well as materials systems, multicolor composition inside the single-particle (individual) can provide labeling possibility with multiple fluorescence outcomes based on colors and emission wavelengths. Moreover, tunable sizes of the fluorescent polymer particles in the region of nanometer and micrometer lengthscale can provide the possibility of labeling based on the full spectrum of size. Also, besides the size tunability and color-combination of the single-particle, the one-level assembly of the monochromatic and size-tuned nanoparticles and microparticles can form the platform of a single assembly particle with a wide variety of fluorescence functions. Furthermore, not only the one-level assembly but the multilevel assembly of the multiscale and multicolored fluorescent nanoparticles and microparticles can form the hierarchical fluorescent platform. Microfluidics reaction techniques are highly promising for the formation of hierarchically structured particle networks for optical labeling. Multiscale polymer particles, from

nanoscale particles to mesoscale assemblies and microscale particles, can be generated by varying various parameters in a microfluidics flow setup.^[67,102,159,181–182] Likewise, a broad range of color-coded polymer particles can be obtained by varying similar types of parameters with color combinations in droplets and particles through microfluidics.^[42,67,176,181,183] A general concept for the continuous formation of color-coded particles is shown in **Figure 10A**. The combination of separately synthesized size and color-tunable polymer particles can be useful for the multilabeling purpose. Color is a significant barcode or marker in the particles for labeling purposes.^[111,184–186] Similarly, the size of the particles also reveals diverse information during labeling.^[36,187–188] In a first set, for instance, five different nanoscale particles of the same color and different sizes can be used for labeling. Similarly, five different nanoparticles of different colors but the same size can be used as another set. Progressively, five different nanoparticles of different colors and different sizes can be used for the multilabeling purpose. Similar to nanoparticles, the color and size-coding with microscale polymer particles can also be performed. Furthermore, the combination of size and color-tuned nanoscale particles with size and color-tuned microscale polymer particles provides a multiscale and multicolored hierarchical labeling approach (**Figure 10B**).

The formation of a large number of safely distinguishable labels can be generated based on color-coding mainly. The red-green-blue (RGB) color system can provide a large variety of color combinations (**Figure 10C**). Commercial availability of a wide range of colored fluorescent dyes can be introduced to the particles via microfluidics flow synthesis of particles. In reality, the automated production of large amounts of micro barcode particles of programmable composition is still a challenge. Much easier is the integration of small particles into larger particles without any spatial order. This strategy can be realized even with spherical particles and does not demand anisotropic (shape-controlled) particles. This strategy is based on the approach of a hierarchical combinatorial integration of nanoparticles by nested embedding. In the first step, a combination of a low number of base colors can be used. From this, a medium-sized set of single particles can be generated, for example, 125 different types in the case of three base colors in five different concentrations. In the second step, these particles are integrated into one larger particle. In this way, an integrated hierarchical network based on the colors can be obtained. The number of addressable combinations can be further enhanced if a third level of hierarchical organization is introduced (**Figure 10C**). Integration of three of the secondary formed composed particles with three elementary particles each leads to an extensive combinatorial multiplicity. The purpose of the conceptual development of the hierarchical network based on the size and color-tuned fluorescent polymer particles is to provide barcoding possibilities for various material systems in the industrial productions of various materials.

8. Summary and Outlook

Overall, this progress report mainly summarizes and reviews the experimental research work from the authors' laboratory

regarding multiscale and multicolored fluorescent polymer particles via microfluidic supported syntheses. In general, fluorescent materials are widely known for labeling and imaging applications. Also, recent advancements in the development of sophisticated optical microscopic techniques can allow analyzing the ultimate detection limit at the single-molecule level. While molecular labeling based on green fluorescent proteins, fluorescent antibodies, fluorescent nucleobases, and free fluorescent dyes are versatile for biological systems, the labeling with particles is also very promising for the biological systems as well as materials systems during the industrial productions of materials. As far as particle-based fluorescent labeling is considered, fluorescent quantum dots are highly versatile due to their superior photostability and brightness. However, their toxicity to the biological systems is a major hindrance to their widespread and sustained uses. To address such concern, fluorescent polymer particles are highly promising. Dye-doped fluorescent polymer particles can provide biocompatibility, brightness, and multicolored variability, as well as protect embedded dyes against photobleaching and chemical/photo-degradation during labeling applications. However, synthesizing the multifunctional, uniform, stable, and reproducible fluorescent polymer particles is challenging. Here, we reviewed the synthesis strategies that we have applied during the research from our laboratory regarding multiscale and multicolored fluorescent polymer particles.

Nanoscale fluorescent PMMA particles were developed with a size range of 60–550 nm by incorporating dyes through semi-microfluidic emulsion polymerization as a model fluorescent polymer nanoparticle system. Moreover, by applying various methods such as nanoprecipitation, much smaller polymer nanoparticles of size range down to 10 nm can also be synthesized. Noncovalent dispersion of dyes shows bright fluorescence, but a concern of leaking or aggregation-caused quenching can be realized. Therefore, a model process for covalent linking of fluorescent dye to the polymer nanoparticle network has been developed for long-term stability purposes. While noncovalent and covalent linking of dyes has been linked in the interior of nanoparticles, their attachment or linking were also engineered at the surface and interface. Four different types of dye linking strategies with polymer nanoparticle networks were highlighted with PMMA nanoparticles as a model system because of their ease of polymerization process and formation. Considering the rich properties of polymers such as mechanical strength, elasticity, swellability, etc., other types of biocompatible polymeric systems need to be developed in future endeavors for real applications. Like the emulsion polymerization approach that has been considered here, other types of polymerization processes such as miniemulsion polymerization, suspension polymerization, etc. can be efficiently applied to bind the fluorophores with polymer networks. Also, multiple types of fluorescent dyes can be links to the polymer network for energy transfer mechanisms such as FRET that works based on donor-acceptor distance dependency.^[177]

Similar to nanoscale fluorescent polymer particles, the microparticles of various wetting properties were developed with a size range of 30–800 μm via photopolymerization in droplet microfluidics. The control of tunable size

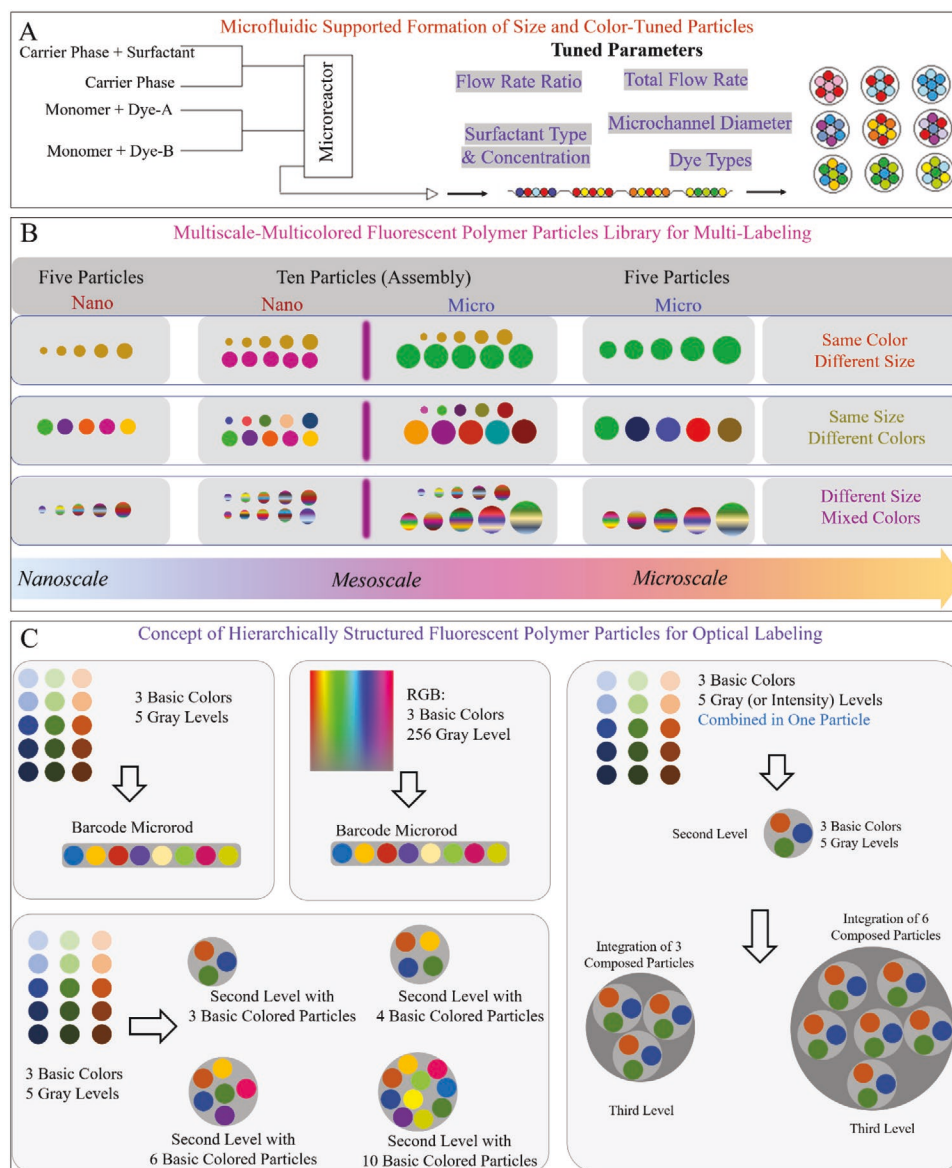


Figure 10. Size and color-tuned hierarchical library of fluorescent polymer particles. A) A basic microfluidic combinatorial scheme for the continuous generation of colored polymer particles by altering various parameters. B) Schematic overview of the multiscale multicolored polymer particles for labeling. A case of 5 particles for the individual nanoparticles and microparticles, as well as ten particles for the assembly particles, has been considered for possible size and color combinations. C) Concept of the hierarchically structured polymer particles for the extensive possibility of color combinations.

resulted by controlling flow rates, flow rate ratios, surfactant concentrations, and microfluidic channel diameter. The microfluidic automated setup has provided a large possibility spectrum of color combinations and size tunability in a continuous flow at the single-step platform. Here, hydrophobic PTPGDA and hydrophilic polyacrylamide microparticles were fabricated with systematic control over their size and color variabilities. Similarly, other types of polymeric systems need to be explored with better control over their structural and interfacial properties. The incorporation of the dyes in a single type of polymer nanoparticle network can combine the softness-related properties of the polymer and brightness-related properties of fluorophore. But, when two or more different types of fluorescent polymer particles can be assembled, then they create a novel

type of hybrid property that is not possible to harvest by a singular type of polymer. Therefore, with the motivation to develop the synthesis procedure for assembly particles, a model system of nanoparticle-nanoparticle assembly and nanoparticle-microparticle assemblies were developed. The assembly process based on polymer particles and fluorophores based on size and color combinations can create an extensive hierarchical labeling platform.

Despite certain types of polymeric materials are considered biocompatible, their characteristics of biocompatibility during real applications to the human body is needed to be explored through research efforts in future endeavors for completely safe uses. In this regard, the development of fluorescent polymer particles based on resorbable polymers containing

lactide, glycolide, ϵ -caprolactone, and trimethylene carbonate needs to be fabricated. When using as sustained fluorescent labels, the network of the fluorescent polymer particles should be stable against light and chemical environments for a long time. But, in the future, an important criterion concerning the environment, living nature, and the intention for realizing closed loops for material processing, the labeling materials have to become equipped with a purpose-adapted biodegradability. The selection of bio- and environmental-compatible dyes is much easier without the recent additional and application-specific challenges for the chemical properties and stability of labeling dyes. The de-coupling between the optical function and the interface to the outside world by the particle-matrix and particle surface allows to choosing dyes with suited biodegradability. In contrast to inorganic materials, it is not difficult to construct the polymer matrix by materials that can be decomposed under natural conditions. For this purpose, ester-based or amide-based polymer materials can be used, in the future, which are synthesized from re-growing materials and can be degraded for re-cycling by natural hydrolases or microorganisms. Besides biological applications as the labeling of cells or tissues, there is to expect a large future field for the application of the soft optical colored particles for material labeling, process monitoring, material flow and recycling, and all kinds of product labeling. The particles can be embedded in all types of plastics and composite materials, fibers for textiles, packaging materials, housing elements, papers, and encapsulation materials for electronics, for example. They can be dispersed inside liquids as process water and wastewater, inside fuels, and all kinds of process liquids.

In general, all needed fluorescent particles can be produced in direct connection with their application. A small compact device or module is sufficient for the generation of particle sets of the desired labeling function. A universal type of programmable particle generator can be integrated into all versions of production and distribution processes. These devices are based on a wide-ranging generation principle for the particles and a very small number of basic materials. The particle synthesis is always combining a standard synthesis method and a small set of standard reactants with a high variability of the dye composition. This variability can be realized by the variation of flow rates in a microfluidic device. The basic principle is the computer-control of flow rates during the particle synthesis for achieving specific labeling.

Acknowledgements

Financial support by the German Research Foundation (Deutsche Forschungsgemeinschaft—DFG) (Projects KO1403/39-1 and KO1403-39-3) is gratefully acknowledged. The authors would also like to thank all unknown reviewers of this paper. Their comments and important suggestions were very helpful to significantly improve the manuscript before publication.

Open access funding enabled and organized by Projekt DEAL.

Conflict of Interest

The authors declare no conflict of interest.

Keywords

fluorescent polymer particles, imaging, labeling, microfluidics, size and color tunability

Received: December 21, 2020

Revised: February 27, 2021

Published online: May 4, 2021

- [1] J. L. West, N. J. Halas, *Annu. Rev. Biomed. Eng.* **2003**, *5*, 285.
- [2] Y. Jiang, K. Pu, *Acc. Chem. Res.* **2018**, *51*, 1840.
- [3] L. Xue, I. A. Karpenko, J. Hiblot, K. Johnsson, *Nat. Chem. Biol.* **2015**, *11*, 917.
- [4] D. Jung, K. Min, J. Jung, W. Jang, Y. Kwon, *Mol. BioSyst.* **2013**, *9*, 862.
- [5] J.-M. Swiecicki, J. T. Santana, B. Imperiali, *Cell Chem. Biol.* **2020**, *27*, 245.
- [6] H. L. Chan, L. Lyu, J. Aw, W. Zhang, J. Li, H.-H. Yang, H. Hayashi, S. Chiba, B. Xing, *ACS Chem. Biol.* **2018**, *13*, 1890.
- [7] H. Sahoo, *RSC Adv.* **2012**, *2*, 7017.
- [8] H. Wang, X. Ji, Z. Li, F. Huang, *Adv. Mater.* **2017**, *29*, 1606117.
- [9] M. Yu, P. Zhang, B. P. Krishnan, H. Wang, Y. Gao, S. Chen, R. Zeng, J. Cui, J. Chen, *Adv. Funct. Mater.* **2018**, *28*, 1804759.
- [10] C. Li, A. G. Tebo, A. Gautier, *Int. J. Mol. Sci.* **2017**, *18*, 1473.
- [11] K. M. Dean, A. E. Palmer, *Nat. Chem. Biol.* **2014**, *10*, 512.
- [12] E. Kozma, P. Kele, *Org. Biomol. Chem.* **2019**, *17*, 215.
- [13] O. S. Wolfbeis, *Chem. Soc. Rev.* **2015**, *44*, 4743.
- [14] A. G. Tebo, B. Moeyaert, M. Thauvin, I. Carlon-Andres, D. Böken, M. Volovitch, S. Padilla-Parra, P. Dedecker, S. Vriz, A. Gautier, *Nat. Chem. Biol.* **2021**, *17*, 30.
- [15] L. D. Lavis, R. T. Raines, *ACS Chem. Biol.* **2014**, *9*, 855.
- [16] K. Umezawa, Y. Nakamura, H. Makino, D. Citterio, K. Suzuki, *J. Am. Chem. Soc.* **2008**, *130*, 1550.
- [17] X. Sun, Y. Wang, Y. Lei, *Chem. Soc. Rev.* **2015**, *44*, 8019.
- [18] H.-S. Peng, D. T. Chiu, *Chem. Soc. Rev.* **2015**, *44*, 4699.
- [19] H. Kobayashi, M. Ogawa, R. Alford, P. L. Choyke, Y. Urano, *Chem. Rev.* **2010**, *110*, 2620.
- [20] G. Ulrich, R. Ziessel, A. Harriman, *Angew. Chem., Int. Ed.* **2008**, *47*, 1184.
- [21] E. Heyer, P. Lory, J. Leprince, M. Moreau, A. Romieu, M. Guardigli, A. Roda, R. Ziessel, *Angew. Chem., Int. Ed.* **2015**, *54*, 2995.
- [22] L. D. Lavis, R. T. Raines, *ACS Chem. Biol.* **2008**, *3*, 142.
- [23] R. Strack, *Nat. Methods* **2021**, *18*, 30.
- [24] J. B. Grimm, B. P. English, J. Chen, J. P. Slaughter, Z. Zhang, A. Revyakin, R. Patel, J. J. Macklin, D. Normanno, R. H. Singer, T. Lionnet, L. D. Lavis, *Nat. Methods* **2015**, *12*, 244.
- [25] J. B. Grimm, A. K. Muthusamy, Y. Liang, T. A. Brown, W. C. Lemon, R. Patel, R. Lu, J. J. Macklin, P. J. Keller, N. Ji, L. D. Lavis, *Nat. Methods* **2017**, *14*, 987.
- [26] J. B. Grimm, A. N. Tkachuk, L. Xie, H. Choi, B. Mohar, N. Falco, K. Schaefer, R. Patel, Q. Zheng, Z. Liu, J. Lippincott-Schwartz, T. A. Brown, L. D. Lavis, *Nat. Methods* **2020**, *17*, 815.
- [27] E. C. Jensen, *Anat. Rec.* **2012**, *295*, 2031.
- [28] V. Saxena, M. Sadoqi, J. Shao, *J. Pharm. Sci.* **2003**, *92*, 2090.
- [29] I. L. Medintz, H. T. Uyeda, E. R. Goldman, H. Mattoussi, *Nat. Mater.* **2005**, *4*, 435.
- [30] M. A. Walling, J. A. Novak, J. R. E. Shepard, *Int. J. Mol. Sci.* **2009**, *10*, 441.
- [31] M. Bruchez, M. Moronne, P. Gin, S. Weiss, A. P. Alivisatos, *Science* **1998**, *281*, 2013.
- [32] O. T. Bruns, T. S. Bischof, D. K. Harris, D. Franke, Y. Shi, L. Riedemann, A. Bartelt, F. B. Jaworski, J. A. Carr, C. J. Rowlands, M. W. B. Wilson, O. Chen, H. Wei, G. W. Hwang, D. M. Montana,

- I. Coropceanu, O. B. Achorn, J. Kloepper, J. Heeren, P. T. C. So, D. Fukumura, K. F. Jensen, R. K. Jain, M. G. Bawendi, *Nat. Biomed. Eng.* **2017**, *1*, 0056.
- [33] L. Wang, M. Hasanzadeh Kafshgari, M. Meunier, *Adv. Funct. Mater.* **2020**, *30*, 2005400.
- [34] K. M. Tsoi, Q. Dai, B. A. Alman, W. C. W. Chan, *Acc. Chem. Res.* **2013**, *46*, 662.
- [35] N. Visaveliya, C. Hoffmann, A. Gross, E. Tauscher, U. Ritter, J. M. Koehler, *Nanotechnol. Rev.* **2016**, *5*, 259.
- [36] A. Reisch, A. S. Klymchenko, *Small* **2016**, *12*, 1968.
- [37] L. Delafresnaye, J. P. Hooker, C. W. Schmitt, L. Barner, C. Barner-Kowollik, *Macromolecules* **2020**, *53*, 5826.
- [38] F. Tronc, M. Li, J. Lu, M. A. Winnik, B. L. Kaul, J.-C. Graciet, *J. Polym. Sci., Part A: Polym. Chem.* **2003**, *41*, 766.
- [39] S. G. Liu, N. Li, Y. Ling, B. H. Kang, S. Geng, N. B. Li, H. Q. Luo, *Langmuir* **2016**, *32*, 1881.
- [40] T. Repenko, A. Rix, S. Ludwanowski, D. Go, F. Kiessling, W. Lederle, A. J. C. Kuehne, *Nat. Commun.* **2017**, *8*, 470.
- [41] M. P. Robin, R. K. O'Reilly, *Polym. Int.* **2015**, *64*, 174.
- [42] N. Visaveliya, J. M. Kohler, *J. Mater. Chem. C* **2015**, *3*, 844.
- [43] Y. Gu, J. Zhao, J. A. Johnson, *Angew. Chem., Int. Ed.* **2020**, *59*, 5022.
- [44] M. A. C. Stuart, W. T. S. Huck, J. Genzer, M. Muller, C. Ober, M. Stamm, G. B. Sukhorukov, I. Szleifer, V. V. Tsukruk, M. Urban, F. Winnik, S. Zauscher, I. Luzinov, S. Minko, *Nat. Mater.* **2010**, *9*, 101.
- [45] A. Bordat, T. Boissenot, J. Nicolas, N. Tsapis, *Adv. Drug Delivery Rev.* **2019**, *138*, 167.
- [46] S. Mura, J. Nicolas, P. Couvreur, *Nat. Mater.* **2013**, *12*, 991.
- [47] A. Musyanovych, K. Landfester, *Macromol. Biosci.* **2014**, *14*, 458.
- [48] M. Zhu, D. Lu, S. Wu, Q. Lian, W. Wang, A. H. Milani, Z. Cui, N. T. Nguyen, M. Chen, L. A. Lyon, D. J. Adlam, A. J. Freemont, J. A. Hoyland, B. R. Saunders, *ACS Macro Lett.* **2017**, *6*, 1245.
- [49] J.-M. Rabanel, V. Adibnia, S. F. Tehrani, S. Sanche, P. Hildgen, X. Banquy, C. Ramassamy, *Nanoscale* **2019**, *11*, 383.
- [50] A. S. Klymchenko, F. Liu, M. Collot, N. Anton, *Adv. Healthcare Mater.* **2021**, *10*, 2001289.
- [51] A. Reisch, K. Trofymchuk, A. Runser, G. Fleith, M. Rawiso, A. S. Klymchenko, *ACS Appl. Mater. Interfaces* **2017**, *9*, 43030.
- [52] B. Andreiuk, A. Reisch, E. Bernhardt, A. S. Klymchenko, *Chem. Asian J.* **2019**, *14*, 836.
- [53] R. Karnik, F. Gu, P. Basto, C. Cannizzaro, L. Dean, W. Kyei-Manu, R. Langer, O. C. Farokhzad, *Nano Lett.* **2008**, *8*, 2906.
- [54] W. Li, L. Zhang, X. Ge, B. Xu, W. Zhang, L. Qu, C.-H. Choi, J. Xu, A. Zhang, H. Lee, D. A. Weitz, *Chem. Soc. Rev.* **2018**, *47*, 5646.
- [55] J. H. Kim, T. Y. Jeon, T. M. Choi, T. S. Shim, S.-H. Kim, S.-M. Yang, *Langmuir* **2014**, *30*, 1473.
- [56] C. A. Serra, Z. Chang, *Chem. Eng. Technol.* **2008**, *31*, 1099.
- [57] J. M. Kohler, S. N. Li, A. Knauer, *Chem. Eng. Technol.* **2013**, *36*, 887.
- [58] Y. Ding, P. D. Howes, A. J. deMello, *Anal. Chem.* **2020**, *92*, 132.
- [59] S. Marre, K. F. Jensen, *Chem. Soc. Rev.* **2010**, *39*, 1183.
- [60] J. I. Park, A. Saffari, S. Kumar, A. Günther, E. Kumacheva, *Annu. Rev. Mater. Res.* **2010**, *40*, 415.
- [61] L. Shang, Y. Cheng, Y. Zhao, *Chem. Rev.* **2017**, *117*, 7964.
- [62] A. Suesa-Ngam, P. D. Howes, M. Srisa-Art, A. J. deMello, *Chem. Commun.* **2019**, *55*, 9895.
- [63] A. B. Theberge, F. Courtois, Y. Schaeferli, M. Fischlechner, C. Abell, F. Hollfelder, W. T. S. Huck, *Angew. Chem., Int. Ed.* **2010**, *49*, 5846.
- [64] S. Q. Xu, Z. H. Nie, M. Seo, P. Lewis, E. Kumacheva, H. A. Stone, P. Garstecki, D. B. Weibel, I. Gitlin, G. M. Whitesides, *Angew. Chem., Int. Ed.* **2005**, *44*, 724.
- [65] N. Visaveliya, S. Lenke, J. M. Kohler, *ACS Appl. Mater. Interfaces* **2015**, *7*, 10742.
- [66] N. R. Visaveliya, C. W. Leishman, K. Ng, N. Yehya, N. Tobar, D. M. Eisele, J. M. Köhler, *Adv. Mater. Interfaces* **2017**, *4*, 1700929.
- [67] N. Visaveliya, J. M. Köhler, *Small* **2015**, *11*, 6435.
- [68] C. Cilliers, I. Nessler, N. Christodolu, G. M. Thurber, *Mol. Pharmaceutics* **2017**, *14*, 1623.
- [69] Z. Cheng, E. Kuru, A. Sachdeva, M. Vendrell, *Nat. Rev. Chem.* **2020**, *4*, 275.
- [70] W. Xu, K. M. Chan, E. T. Kool, *Nat. Chem.* **2017**, *9*, 1043.
- [71] R. Y. Tsien, *Angew. Chem., Int. Ed.* **2009**, *48*, 5612.
- [72] I. Segal, D. Nachmias, A. Konig, A. Alon, E. Arbely, N. Elia, *BMC Biol.* **2020**, *18*, 5.
- [73] A. Bhirde, J. Xie, M. Swierczewska, X. Chen, *Nanoscale* **2011**, *3*, 142.
- [74] M. C. Belanger, M. Zhuang, A. G. Ball, K. H. Richey, C. A. DeRosa, C. L. Fraser, R. R. Pompano, *Biomater. Sci.* **2020**, *8*, 1897.
- [75] T. F. Abelha, C. A. Dreiss, M. A. Green, L. A. Dailey, *J. Mater. Chem. B* **2020**, *8*, 592.
- [76] S. Wen, J. Zhou, K. Zheng, A. Bednarkiewicz, X. Liu, D. Jin, *Nat. Commun.* **2018**, *9*, 2415.
- [77] S. Zhang, R. Liu, Q. Cui, Y. Yang, Q. Cao, W. Xu, L. Li, *ACS Appl. Mater. Interfaces* **2017**, *9*, 44134.
- [78] M. Zhang, L. Vojtech, Z. Ye, F. Hladik, E. Nance, *ACS Appl. Nano Mater.* **2020**, *3*, 7211.
- [79] C. Wu, Y. Zheng, C. Szymanski, J. McNeill, *J. Phys. Chem. C* **2008**, *112*, 1772.
- [80] Y. C. Simon, S. Bai, M. K. Sing, H. Dietsch, M. Achermann, C. Weder, *Macromol. Rapid Commun.* **2012**, *33*, 498.
- [81] S. Bhattacharyya, S. Prashanthi, P. R. Bangal, A. Patra, *J. Phys. Chem. C* **2013**, *117*, 26750.
- [82] M. J. Webber, E. A. Appel, E. W. Meijer, R. Langer, *Nat. Mater.* **2015**, *15*, 13.
- [83] E. E. Stache, V. Kottisch, B. P. Fors, *J. Am. Chem. Soc.* **2020**, *142*, 4581.
- [84] Y. Gu, J. Zhao, J. A. Johnson, *Trends Chem.* **2019**, *1*, 318.
- [85] P. Salas-Ambrosio, A. Tronnet, P. Verhaeghe, C. Bonduelle, *Biomacromolecules* **2021**, *22*, 57.
- [86] A. S. Carlini, L. Adamiak, N. C. Gianneschi, *Macromolecules* **2016**, *49*, 4379.
- [87] J. J. Kaufman, R. Ottman, G. Tao, S. Shabahang, E.-H. Banaei, X. Liang, S. G. Johnson, Y. Fink, R. Chakrabarti, A. F. Abouraddy, *Proc. Natl. Acad. Sci. USA* **2013**, *110*, 15549.
- [88] M. Elsbahy, G. S. Heo, S.-M. Lim, G. Sun, K. L. Wooley, *Chem. Rev.* **2015**, *115*, 10967.
- [89] T. Tamai, M. Watanabe, H. Maeda, K. Mizuno, *J. Polym. Sci., Part A: Polym. Chem.* **2008**, *46*, 1470.
- [90] Z. Song, E. S. Daniels, E. D. Sudol, J. F. Gilchrist, A. Klein, M. S. El-Aasser, *J. Appl. Polym. Sci.* **2013**, *127*, 2635.
- [91] D. Qi, X. Yang, W. Huang, *Polym. Int.* **2007**, *56*, 208.
- [92] Y. Wu, Y. Li, J. Xu, D. Wu, *J. Mater. Chem. B* **2014**, *2*, 5837.
- [93] A. Gharieh, S. Khoee, A. R. Mahdavian, *Adv. Colloid Interface Sci.* **2019**, *269*, 152.
- [94] V. Chaudhary, S. Sharma, *J. Polym. Res.* **2019**, *26*, 102.
- [95] B. Volkmer, M. Heinemann, *PLoS One* **2011**, *6*, 23126.
- [96] N. Hoshyar, S. Gray, H. Han, G. Bao, *Nanomedicine* **2016**, *11*, 673.
- [97] Y.-H. You, A. Biswas, A. T. Nagaraja, J.-H. Hwang, G. L. Coté, M. J. McShane, *ACS Appl. Mater. Interfaces* **2019**, *11*, 14286.
- [98] F. Progzatzky, M. J. Dallman, C. L. Celso, *Interface Focus* **2013**, *3*, 20130001.
- [99] A. Bunschoten, D. M. van Willigen, T. Buckle, N. S. van den Berg, M. M. Welling, S. J. Spa, H.-J. Wester, F. W. B. van Leeuwen, *Bioconjugate Chem.* **2016**, *27*, 1253.
- [100] K. S. Hettie, J. L. Klockow, T. E. Glass, F. T. Chin, *Anal. Chem.* **2019**, *91*, 3110.
- [101] D. Geißler, C. Gollwitzer, A. Sikora, C. Minelli, M. Krumrey, U. Resch-Genger, *Anal. Methods* **2015**, *7*, 9785.
- [102] N. Visaveliya, J. M. Kohler, *ACS Appl. Mater. Interfaces* **2014**, *6*, 11254.
- [103] N. Visaveliya, J. M. Köhler, *Langmuir* **2014**, *30*, 12180.
- [104] B. Amoyav, O. Benny, *Appl. Nanosci.* **2018**, *8*, 905.

- [105] A. Badasyan, A. Mavrič, I. Kralj Cigić, T. Bencik, M. Valant, *Soft Matter* **2018**, *14*, 4735.
- [106] S. Shashkova, M. C. Leake, *Biosci. Rep.* **2017**, *37*, BSR20170031.
- [107] D. R. Walt, *Anal. Chem.* **2013**, *85*, 1258.
- [108] G. Sun, M. Y. Berezin, J. Fan, H. Lee, J. Ma, K. Zhang, K. L. Wooley, S. Achilefu, *Nanoscale* **2010**, *2*, 548.
- [109] Z. Lin, H. Wang, M. Yu, X. Guo, C. Zhang, H. Deng, P. Zhang, S. Chen, R. Zeng, J. Cui, J. Chen, *J. Mater. Chem. C* **2019**, *7*, 11515.
- [110] K. P. Yuet, D. K. Hwang, R. Haghgooie, P. S. Doyle, *Langmuir* **2010**, *26*, 4281.
- [111] Y. Zhao, Y. Cheng, L. Shang, J. Wang, Z. Xie, Z. Gu, *Small* **2015**, *11*, 151.
- [112] Y. Song, J. Hormes, C. S. S. R. Kumar, *Small* **2008**, *4*, 698.
- [113] D. Cambié, C. Bottecchia, N. J. W. Straathof, V. Hessel, T. Noël, *Chem. Rev.* **2016**, *116*, 10276.
- [114] S. Xu, Z. Nie, M. Seo, P. Lewis, E. Kumacheva, H. A. Stone, P. Garstecki, D. B. Weibel, I. Gitlin, G. M. Whitesides, *Angew. Chem., Int. Ed.* **2005**, *44*, 724.
- [115] H. Song, D. L. Chen, R. F. Ismagilov, *Angew. Chem., Int. Ed.* **2006**, *45*, 7336.
- [116] P. Garstecki, M. J. Fuerstman, H. A. Stone, G. M. Whitesides, *Lab Chip* **2006**, *6*, 437.
- [117] C. H. Meredith, P. G. Moerman, J. Groenewold, Y.-J. Chiu, W. K. Kegel, A. van Blaaderen, L. D. Zarzar, *Nat. Chem.* **2020**, *12*, 1136.
- [118] K. Doufène, C. Tourné-Péteilh, P. Etienne, A. Aubert-Pouëssel, *Langmuir* **2019**, *35*, 12597.
- [119] A. Z. Nelson, B. Kundukad, W. K. Wong, S. A. Khan, P. S. Doyle, *Proc. Natl. Acad. Sci. USA* **2020**, *117*, 5671.
- [120] J. K. Nunes, S. S. H. Tsai, J. Wan, H. A. Stone, *J. Phys. D: Appl. Phys.* **2013**, *46*, 114002.
- [121] J. M. Koehler, F. Moeller, S. Schneider, P. M. Guenther, A. Albrecht, G. A. Gross, *Chem. Eng. J.* **2011**, *167*, 688.
- [122] F. He, M.-J. Zhang, W. Wang, Q.-W. Cai, Y.-Y. Su, Z. Liu, Y. Faraj, X.-J. Ju, R. Xie, L.-Y. Chu, *Adv. Mater. Technol.* **2019**, *4*, 1800687.
- [123] J. Wang, Y. Li, X. Wang, J. Wang, H. Tian, P. Zhao, Y. Tian, Y. Gu, L. Wang, C. Wang, *Micromachines* **2017**, *8*, 22.
- [124] N. Visaveliya, S. Lenke, A. Gross, J. M. Kohler, *Chem. Eng. Technol.* **2015**, *38*, 1144.
- [125] T. Behnke, C. Würth, E.-M. Laux, K. Hoffmann, U. Resch-Genger, *Dyes Pigm.* **2012**, *94*, 247.
- [126] C. J. Martínez Rivas, M. Tarhini, W. Badri, K. Miladi, H. Greige-Gerges, Q. A. Nazari, S. A. Galindo Rodríguez, R. Á. Román, H. Fessi, A. Elaissari, *Int. J. Pharm.* **2017**, *532*, 66.
- [127] A. Alshamsan, *Saudi Pharm. J.* **2014**, *22*, 219.
- [128] V. Rosiuk, A. Runser, A. Klymchenko, A. Reisch, *Langmuir* **2019**, *35*, 7009.
- [129] S. Bhargava, J. J. H. Chu, S. Valiyaveetil, *ACS Omega* **2018**, *3*, 7663.
- [130] K. Li, B. Liu, *Chem. Soc. Rev.* **2014**, *43*, 6570.
- [131] A. Reisch, A. Runser, Y. Arntz, Y. Mély, A. S. Klymchenko, *ACS Nano* **2015**, *9*, 5104.
- [132] A. Reisch, D. Heimbürger, P. Ernst, A. Runser, P. Didier, D. Dujardin, A. S. Klymchenko, *Adv. Funct. Mater.* **2018**, *28*, 1805157.
- [133] S. Schubert, J. J. T. Delaney, U. S. Schubert, *Soft Matter* **2011**, *7*, 1581.
- [134] A. Wagh, S. Y. Qian, B. Law, *Bioconjugate Chem.* **2012**, *23*, 981.
- [135] S. Mourdikoudis, R. M. Pallares, N. T. K. Thanh, *Nanoscale* **2018**, *10*, 12871.
- [136] N. R. Visaveliya, J. M. Köhler, *Biomacromolecules* **2018**, *19*, 1047.
- [137] A. Gupta, H. B. Eral, T. A. Hatton, P. S. Doyle, *Soft Matter* **2016**, *12*, 2826.
- [138] I. N. Kurniasih, H. Liang, P. C. Mohr, G. Khot, J. P. Rabe, A. Mohr, *Langmuir* **2015**, *31*, 2639.
- [139] B. R. Bzdek, J. P. Reid, J. Malila, N. L. Prisle, *Proc. Natl. Acad. Sci. USA* **2020**, *117*, 8335.
- [140] L. A. Puentes-Vara, K. M. Gregorio-Jauregui, A. M. Bolarín, M. E. Navarro-Clemente, H. J. Dorantes, M. Corea, *J. Nanopart. Res.* **2016**, *18*, 212.
- [141] H. Heinz, C. Pramanik, O. Heinz, Y. Ding, R. K. Mishra, D. Marchon, R. J. Flatt, I. Estrela-Lopis, J. Llop, S. Moya, R. F. Ziolo, *Surf. Sci. Rep.* **2017**, *72*, 1.
- [142] A. S. Klymchenko, *Acc. Chem. Res.* **2017**, *50*, 366.
- [143] T. Zhao, T. Masuda, E. Miyoshi, M. Takai, *Anal. Chem.* **2020**, *92*, 13271.
- [144] A. Wagh, F. Jyoti, S. Mallik, S. Qian, E. Leclerc, B. Law, *Small* **2013**, *9*, 2129.
- [145] J. M. Kürner, I. Klimant, C. Krause, E. Pringsheim, O. S. Wolfbeis, *Anal. Biochem.* **2001**, *297*, 32.
- [146] I. Khalin, D. Heimbürger, N. Melnychuk, M. Collot, B. Groschup, F. Hellal, A. Reisch, N. Plesnila, A. S. Klymchenko, *ACS Nano* **2020**, *14*, 9755.
- [147] Y. Xue, J. Lee, H.-J. Kim, H.-J. Cho, X. Zhou, Y. Liu, P. Tebon, T. Hoffman, M. Qu, H. Ling, X. Jiang, Z. Li, S. Zhang, W. Sun, S. Ahadian, M. R. Dokmeci, K. Lee, A. Khademhosseini, *ACS Appl. Bio Mater.* **2020**, *3*, 6908.
- [148] C. Grazon, J. Rieger, R. Méallet-Renault, B. Charleux, G. Clavier, *Macromolecules* **2013**, *46*, 5167.
- [149] H. Gao, W. Shi, L. B. Freund, *Proc. Natl. Acad. Sci. USA* **2005**, *102*, 9469.
- [150] J. A. Champion, S. Mitragotri, *Proc. Natl. Acad. Sci. USA* **2006**, *103*, 4930.
- [151] P. Kolhar, A. C. Anselmo, V. Gupta, K. Pant, B. Prabhakar Pandian, E. Ruoslahti, S. Mitragotri, *Proc. Natl. Acad. Sci. USA* **2013**, *110*, 10753.
- [152] N. Visaveliya, J. M. Kohler, *Macromol. Chem. Phys.* **2015**, *216*, 1212.
- [153] J. Mei, N. L. C. Leung, R. T. K. Kwok, J. W. Y. Lam, B. Z. Tang, *Chem. Rev.* **2015**, *115*, 11718.
- [154] H. Qin, J. Huang, H. Liang, J. Lu, *ACS Appl. Mater. Interfaces* **2021**, *13*, 5668.
- [155] A. Reisch, P. Didier, L. Richert, S. Oncul, Y. Arntz, Y. Mély, A. S. Klymchenko, *Nat. Commun.* **2014**, *5*, 4089.
- [156] K. Trofymchuk, A. Reisch, I. Shulov, Y. Mély, A. S. Klymchenko, *Nanoscale* **2014**, *6*, 12934.
- [157] R. Méallet-Renault, A. Hérault, J.-J. Vachon, R. B. Pansu, S. Amigoni-Gerbier, C. Larpent, *Photochem. Photobiol. Sci.* **2006**, *5*, 300.
- [158] D. Vollath, F. D. Fischer, D. Holec, *Beilstein J. Nanotechnol.* **2018**, *9*, 2265.
- [159] N. R. Visaveliya, X. Li, A. Knauer, B. L. V. Prasad, J. M. Köhler, *Macromol. Chem. Phys.* **2017**, *218*, 1700261.
- [160] Á. Szabó, T. Szendi-Szattmári, L. Ujlaky-Nagy, I. Rádi, G. Vereb, J. Szöllösi, P. Nagy, *Biophys. J.* **2018**, *114*, 688.
- [161] A. Simeonov, M. Matsushita, E. A. Juban, E. H. Z. Thompson, T. Z. Hoffman, A. E. Beuscher, M. J. Taylor, P. Wirsching, W. Rettig, J. K. McCusker, R. C. Stevens, D. P. Millar, P. G. Schultz, R. A. Lerner, K. D. Janda, *Science* **2000**, *290*, 307.
- [162] B. N. G. Giepmans, S. R. Adams, M. H. Ellisman, R. Y. Tsien, *Science* **2006**, *312*, 217.
- [163] S. M. Sedlak, L. C. Schendel, H. E. Gaub, R. C. Bernardi, *Sci. Adv.* **2020**, *6*, eaay5999.
- [164] D. Zhou, H. Xiao, F. Meng, S. Zhou, J. Guo, X. Li, X. Jing, Y. Huang, *Bioconjugate Chem.* **2012**, *23*, 2335.
- [165] T. Ji, M. C. Muenker, R. V. L. Papineni, J. W. Harder, D. L. Vizard, W. E. McLaughlin, *Bioconjugate Chem.* **2010**, *21*, 427.
- [166] B. Taskinen, D. Zauner, S. I. Lehtonen, M. Koskinen, C. Thomson, N. Kähkönen, S. Kukkurainen, J. A. E. Määttä, T. O. Ihalainen, M. S. Kulomaa, H. J. Gruber, V. P. Hytönen, *Bioconjugate Chem.* **2014**, *25*, 2233.

- [167] M. V. Rekharsky, T. Mori, C. Yang, Y. H. Ko, N. Selvapalam, H. Kim, D. Sobransingh, A. E. Kaifer, S. Liu, L. Isaacs, W. Chen, S. Moghaddam, M. K. Gilson, K. Kim, Y. Inoue, *Proc. Natl. Acad. Sci. USA* **2007**, *104*, 20737.
- [168] N. Melnychuk, A. S. Klymchenko, *J. Am. Chem. Soc.* **2018**, *140*, 10856.
- [169] L. A. Bawazer, C. S. McNally, C. J. Empson, W. J. Marchant, T. P. Comyn, X. Niu, S. Cho, M. J. McPherson, B. P. Binks, A. deMello, F. C. Meldrum, *Sci. Adv.* **2016**, *2*, 1600567.
- [170] C. W. Visser, T. Kamperman, L. P. Karbaat, D. Lohse, M. Karperien, *Sci. Adv.* **2018**, *4*, eaao1175.
- [171] H. R. Holmes, K. F. Böhringer, *Microsyst. Nanoeng.* **2015**, *1*, 15022.
- [172] B. V. Slaughter, S. S. Khurshid, O. Z. Fisher, A. Khademhosseini, N. A. Peppas, *Adv. Mater.* **2009**, *21*, 3307.
- [173] Y. Sun, D. Nan, H. Jin, X. Qu, *Polym. Test.* **2020**, *81*, 106283.
- [174] N. R. Richbourg, N. A. Peppas, *Prog. Polym. Sci.* **2020**, *105*, 101243.
- [175] D. Pappalardo, T. Mathisen, A. Finne-Wistrand, *Biomacromolecules* **2019**, *20*, 1465.
- [176] N. Visaveliya, A. Knauer, W. Yu, C. A. Serra, J. M. Kohler, *Eur. Polym. J.* **2016**, *80*, 256.
- [177] S. Kundu, S. Bhattacharyya, A. Patra, *Mater. Horiz.* **2015**, *2*, 60.
- [178] D. Genovese, E. Rampazzo, S. Bonacchi, M. Montalti, N. Zaccheroni, L. Prodi, *Nanoscale* **2014**, *6*, 3022.
- [179] B. Jana, S. Bhattacharyya, A. Patra, *Nanoscale* **2016**, *8*, 16034.
- [180] W. Yu, N. Visaveliya, C. A. Serra, J. M. Köhler, S. Ding, M. Bouquey, R. Muller, M. Schmutz, I. Kraus, *Materials* **2019**, *12*, 3921.
- [181] N. Visaveliya, A. Knauer, J. M. Köhler, *Macromol. Chem. Phys.* **2017**, *218*, 1600371.
- [182] J. M. Koehler, N. Visaveliya, A. Knauer, *Nanotechnol. Rev.* **2014**, *3*, 553.
- [183] L. Maggini, D. Bonifazi, *Chem. Soc. Rev.* **2012**, *41*, 211.
- [184] B. Andreiuk, A. Reisch, M. Lindecker, G. Follain, N. Peyri ras, J. G. Goetz, A. S. Klymchenko, *Small* **2017**, *13*, 1701582.
- [185] L. Guo, T. Wang, Z. Wu, J. Wang, M. Wang, Z. Cui, S. Ji, J. Cai, C. Xu, X. Chen, *Adv. Mater.* **2020**, *32*, 2004805.
- [186] G. Tang, L. Chen, Z. Wang, S. Gao, Q. Qu, R. Xiong, K. Braeckmans, S. C. De Smedt, Y. S. Zhang, C. Huang, *Small* **2020**, *16*, 1907586.
- [187] M. Castellarnau, G. L. Szeto, H.-W. Su, T. Tokatlian, J. C. Love, D. J. Irvine, J. Voldman, *Small* **2015**, *11*, 489.
- [188] J.-T. Wang, J. Wang, J.-J. Han, *Small* **2011**, *7*, 1728.



Nikunj Kumar R. Visaveliya studied Chemistry at Sardar Patel University in India. He obtained his doctoral degree from the Technical University of Ilmenau, Germany where he performed research on microfluidic syntheses of multifunctional polymer and composite nano/microparticles for sensing and labeling applications. Currently, he is a postdoctoral researcher at the City College of New York, USA. His research interests are microfluidics and interfacial/functional nanomaterials for biomedical, energy, catalysis, sensing, and labeling applications.



Johann Michael Köhler is a professor and head of the Department of Physical Chemistry and Microreaction Technology at the Technical University of Ilmenau, Germany since 2001. He studied Chemistry in Halle/S. and Jena, Germany, where he was also habilitated in General and Physical Chemistry in 1992. He edited/wrote books on microlithography, microsystem technology, nanotechnology, and sensor technology. His research interests include micro/nanotechnology, synthesis of metallic and polymer complex nanomaterials, as well as the development and application of fluidic microsystems in the fields of Chemistry and Biology.